

South Dakota State University

# Open PRAIRIE: Open Public Research Access Institutional Repository and Information Exchange

---

Electronic Theses and Dissertations

---

2022

## Modeling the Flow and Creep Compliance Properties of Ice-Cream Mixes

Hiran Ranaweera

South Dakota State University, hiransdsu48@gmail.com

Follow this and additional works at: <https://openprairie.sdstate.edu/etd2>



Part of the [Biology Commons](#), [Dairy Science Commons](#), and the [Food Microbiology Commons](#)

---

### Recommended Citation

Ranaweera, Hiran, "Modeling the Flow and Creep Compliance Properties of Ice-Cream Mixes" (2022). *Electronic Theses and Dissertations*. 376.  
<https://openprairie.sdstate.edu/etd2/376>

This Thesis - Open Access is brought to you for free and open access by Open PRAIRIE: Open Public Research Access Institutional Repository and Information Exchange. It has been accepted for inclusion in Electronic Theses and Dissertations by an authorized administrator of Open PRAIRIE: Open Public Research Access Institutional Repository and Information Exchange. For more information, please contact [michael.biondo@sdstate.edu](mailto:michael.biondo@sdstate.edu).

MODELING THE FLOW AND CREEP COMPLIANCE PROPERTIES OF  
ICE-CREAM MIXES

BY

HIRAN RANAWEERA

A thesis submitted in partial fulfilment of the requirements for the

Master of Science

Major in Biological Sciences

Specialization in Dairy Science

South Dakota State University

2022

## THESIS ACCEPTANCE PAGE

H. K. G Hiran

This thesis is approved as a creditable and independent investigation by a candidate for the master's degree and is acceptable for meeting the thesis requirements for this degree.

Acceptance of this does not imply that the conclusions reached by the candidate are necessarily the conclusions of the major department.

Sergio I Martínez-Monteagudo  
Advisor

Date

Joseph P Cassady  
Department Head

Date

Nicole Lounsbury, PhD  
Director, Graduate School

Date

This thesis is dedicated to everyone who helped my journey towards graduation and academic success.

## ACKNOWLEDGEMENTS

I would like to convey my sincere gratitude and thanks to Dr. Sergio Martinez-Monteagudo, my first academic, and thesis advisor, for giving me this opportunity to work with him and for guidance through my research. Also, I thank Dr. Padmanaban Krishnan, my second academic & thesis advisor, for all the support and expertise provided for the research work. Finally, Dr. Joseph P Cassady, my last advisor, for providing the motivation and helping with preparation.

I would also like to thank Dr. Prafulla Salunke and Dr. Heidi Mennenga for serving on my graduate advisory committee. Moreover, I'm grateful for the help from the South Dakota Agricultural Experiment Station for funding portions of my research and Graduate Student Assistantship. Also, Midwest Dairy Association (MDA) for the project support.

I would like to appreciate the help from my lab members, graduate students, and friends for their assistance in and out of the lab. Finally, I would like to honorably mention my parents and family members for their moral support, as well as their encouragement all these years.

## TABLE OF CONTENT

LIST OF TABLES .....	vii
LIST OF FIGURES .....	xiii
ABRIVIATIONS .....	ix
ABSTRACT.....	xii
Chapter 1 .....	1
Introduction and objectives.....	1
<b>1.1 Significance</b> .....	1
<b>1.2 Objectives</b> .....	2
<b>1.3 References</b> .....	3
Chapter 2.....	4
Modeling the viscosity of ice-cream mixes .....	4
<b>2.1 Introduction</b> .....	4
<b>2.2 Materials and methods</b> .....	6
<b>2.2.1 Formulations</b> .....	6
<b>2.2.2 Rheological measurements</b> .....	7
<b>2.2.3 Data analysis</b> .....	7
<b>2.3 Results and discussion</b> .....	10
<b>2.3.1 Flow curves</b> .....	10
<b>2.3.2 Frequency sweeps</b> .....	21
<b>2.4 Conclusions</b> .....	24
<b>2.5 References</b> .....	24
Chapter 3.....	28
Modeling the creep-recovery curves of ice-cream mixes.....	28
<b>3.1 Introduction</b> .....	28
<b>3.2 Materials and methods</b> .....	32
<b>3.2.1 Formulations</b> .....	32
<b>3.2.2 Creep-recovery measurements</b> .....	32
<b>3.2.3 Burger model</b> .....	33
<b>3.3 Results and discussion</b> .....	34
<b>3.3.1 Creep-recovery curves</b> .....	34
<b>3.3.2 Recovery of the system</b> .....	37
<b>3.4 Conclusions</b> .....	43
<b>3.5 References</b> .....	43

**4.1. Overall conclusions ..... 47**

## LIST OF TABLES

<b>Table 2.1.</b> Parameters of the Herschel-Bulkley model for the ice-cream mixes formulated with different protein content.....	15
<b>Table 2.2.</b> Regression analysis of Equation (5) to predict the viscosity as a function of temperature and protein content for ice-cream mixes formulated with milk protein concentrate 80 (MPC80) and whey protein concentrate 80 (WPC80). .....	18
<b>Table 2.3.</b> Relationship between storage module ( $G'$ ) and frequency ( $\omega$ ) for the ice-cream mixes formulated with different protein content. ....	23



## LIST OF FIGURES

<b>Figure 1.</b> Effect of temperature (5, 15, 25, and 35°C) and protein content (4, 10, and 12%) on the logarithmic flow curve of ice-cream mixes: (a) milk protein concentrate 80 (MPC80) and (b) whey protein concentrate 80 (WPC80). .....	12
<b>Figure 2.</b> Effect of temperature and protein on the consistency index ( $mT$ and $mp$ , respectively) of ice-cream mixes containing different protein content: (a) milk protein concentrate 80 (MPC80) and (b) whey protein concentrate 80 (WPC80). .....	13
<b>Figure 3.</b> Joint confidence region of the regression parameters used to predict the viscosity of ice-cream mixes formulated with different protein content. (a) $aT$ vs $mTo$ for MPC80 ( : 4%; :10%; and : 12% of protein content), (b) $aT$ vs $mTo$ for WPC80 ( : 4%; :10%; and : 12% of protein content), (c) $ap$ vs $mpo$ for MPC80 ( : 5°C; : 15°C; : 25°C and : 35°C), and (d) $ap$ vs $mpo$ for WPC80 ( : 5°C; : 15°C; : 25°C and : 35°C). .....	17
<b>Figure 4.</b> Linear relationship between predicted and experimental values of viscosity: (a) milk protein concentrate 80 (MPC80) and (b) whey protein concentrate 80 (WPC80). Blue lines represent the 95% confidence interval band and red lines represent the 95% prediction band.....	19
<b>Figure 5.</b> Predicted viscosity at as a function of temperature and protein content for ice-cream mixes: (a) milk protein concentrate 80 (MPC80) and (b) whey protein concentrate 80 (WPC80). The viscosity values were predicted with Equation (5) using the estimated parameters (Table 1). Shear rate ( $\gamma$ ) was kept constant at 30 s <sup>-1</sup> . .....	20
<b>Figure 6.</b> Frequency sweep analysis of ice-cream mixes formulated containing different protein content: (a) milk protein concentrate 80 (MPC80) and (b) whey protein concentrate 80 (WPC80).....	22
<b>Figure 7.</b> Illustration of a typical creep-recovery curve and dashpot of the Burger model consisted of Maxwell and Kelvin-Voigt models in series. ....	30
<b>Figure 8.</b> Creep-recovery curves of ice-cream mixes formulated with milk protein concentrate 80 (MPC80) at 4, 10, and 12% (a-c). Symbols represents the experimental data while the continuous line represents the Burger model. ....	35
<b>Figure 9.</b> Creep-recovery curves of ice-cream mixes formulated with whey protein concentrate 80 (MPC80) at 4, 10, and 12% (a-c). Symbols represents the experimental data while the continuous line represents the Burger model. ....	36

## ABBREVIATIONS

$A$	gel strength (Pa s <sup>1/2</sup> )
$a_p$	sensitivity parameter for protein
$a_{J_0(p)}$	individual sensitivity parameter accounting for the protein effects
$a_{J_0(T)}$	individual sensitivity parameter accounting for the temperature effects
$a_{J_1(p)}$	individual sensitivity parameter accounting for the protein effects
$a_{J_1(T)}$	individual sensitivity parameter accounting for the temperature effects
$a_T$	sensitivity parameter for temperature
$a_{\lambda_{ret}(T)}$	individual sensitivity parameter accounting for the temperature effects
$a_{\lambda_{ret}(p)}$	individual sensitivity parameter accounting for the protein effects
$a_{n_{oM}(T)}$	individual sensitivity parameter accounting for the temperature effects
$a_{n_{oM}(p)}$	individual sensitivity parameter accounting for the protein effects
$b$	dimensionless parameter
$E$	average absolute percentage of residuals (%)
$G^*$	complex shear module
$G^*_{(\omega)}$	complex module
$G'$	storage module (Pa)
$G''$	loss module (Pa)
$J_0$	instantaneous compliance
$J_1$	compliance associated with the Kelvin-Voigt element
$J_{0(p)}$	regression parameters derived from the protein dependency

$J_{o(T)}$	regression parameters derived from the temperature dependency
$J_{1(p)}$	regression parameters derived from the protein dependency
$J_{1(T)}$	regression parameters derived from the temperature dependency
$J_{o(T,p)}$	regression parameters accounting for the temperature and protein
$J_{1(T,p)}$	regression parameters accounting for the temperature and protein
$J(t)$	compliance as a function of time within the creep phase
$J_{Max}$	maximum deformation
$J_{\infty}$	compliance for the longest time
ICM	ice-cream mixes
MPC	milk protein concentrate
$m_{(T,p)}$	consistency index (Pa s <sup>n</sup> ) influenced by the temperature and protein content
$m_p$	protein dependence on the consistency index
$m_{p0}$	regression parameters
$m_{T0}$	regression parameters
$m_T$	temperature dependence on the consistency index
$n$	flow behavior index
$p$	protein content (%)
$p_r$	reference protein (%)
%R	final recovery of the entire system
$R^2$	coefficient of determination
$R_{Adj}^2$	adjusted coefficient of determination
$t$	test time (s)

$t_1$	time when the stressed was removed
$T$	temperature (°C)
$T_r$	reference temperature (°C)
WPC	whey protein concentrate
$\sigma$	constant stress
$\eta$	viscosity (mPa s)
$\eta_{exp}$	experimental viscosity (mPa s)
$\eta_{pred}$	predicted viscosity (mPa s)
$\eta_o$	yield stress (Pa)
$\eta_{oM}$	residual viscosity of the Maxwell dashpot
$\eta_{oM(T)}$	regression parameters derived from the temperature dependency
$\eta_{oM(p)}$	regression parameters derived from the protein dependency
$\eta_{oM(T,p)}$	regression parameters accounting for the temperature and protein
$\dot{\gamma}$	shear rate (1/s)
$\gamma(t)$	shear deformation
$\delta$	phase angle
$\omega$	frequency (Hz)
$\lambda_{ret}$	retardation time associated with the Kelvin-Voigt element
$\lambda_{ret(T)}$	regression parameters derived from the temperature dependency
$\lambda_{ret(p)}$	regression parameters derived from the protein dependency
$\lambda_{ret(T,p)}$	regression parameters accounting for the temperature and protein

## ABSTRACT

MODELING THE FLOW AND CREEP COMPLIANCE PROPERTIES OF ICE  
CREAM MIXES

HIRAN RENAWEERA

2022

This work documented the influence of the protein source (MPC80 and WPC80), protein content (4-12%), and temperature (5-35°C) on the rheological behavior (flow curve, frequency sweep, and creep-recovery) of ice-cream mixes (ICM). For each protein source, the viscosity of the ICM was satisfactorily modeled ( $R^2 > 0.98$ ,  $R_{adj}^2 > 0.98$ , and  $E < 10\%$ ) using a modified Herschel-Bulkley model, where the consistency index was parameterized to account for the protein and temperature effect. The frequency sweeps of the ICM suggested a dominant viscous gel behavior with increasing protein content. Creep curves were satisfactorily described by the Burger model ( $R^2 > 0.99$ ), while the recovery phase was represented by an empirical model. The percentage of recovery (%R) of the ICM significantly decreased with the protein content.

Keywords: ice-cream mix, modeling viscosity, protein content, frequency sweeps, creep-recovery.

## **Chapter 1**

### **Introduction and objectives**

#### **1.1 Significance**

Over the past few years, powdered proteins have become a popular ingredient in many foods and dietary formulations due to the health benefits associated with their consumption (Hazlett, Schmidmeier, & O'Mahony, 2021). Examples of documented health benefits include promoting satiety, appetite control, and exercise recovery (Tang, O'Connor, & Campbell, 2014; Thomas et al., 2019). As a result, concentrates and isolates (highly concentrated protein fractions) of different protein sources are increasingly used to formulate beverages, snacks, dietary supplements, and desserts. Pea protein, soybean isolates, peanut protein, and dairy proteins are examples of the type of protein used to reformulate such products.

Milk proteins are recognized for their nutritional benefits in the human diet, including bioavailability and absorption rate – fast-absorbing proteins (whey or serum proteins) and slow absorbing proteins (casein micelles) (McGregor & Poppitt, 2013). Additionally, milk proteins are high in essential amino acids – those amino acids that the human body cannot produce naturally (Jana, 2022). Interestingly, the consumption of plant-based proteins has steadily increased over the past few years. Proteins derived from plants are considered as one of the methods for feeding the growing global population. Thus, the incorporation of plant-based proteins within food formulations has attracted a number of consumers, including veganism, fear of health risks on animal-based products, and the concepts like cruelty-free.

Combinations of dairy and plant-based proteins have been used to increase the amount of protein in a number of food formulations. This approach is relatively new, and the impact of the protein blend, concentration, and source of protein on the quality of the resulting product remains largely unknown. Overall, increasing the amount of protein significantly alters the flow characteristics of the entire product, from formulation and mixing to pasteurization and storage. Understanding the role of protein on rheological behavior serves as a foundational step in product and process development. Rheology has been defined as the study of material deformation during and after a given force has been applied (Steffe, 1996). Moreover, rheological analysis is considered an analytical tool to provide fundamental insights into the structure of foods (Ferry, 1980).

Studies on the impact of protein content on the flow characteristics of food formulations are scarce. The hypothesis of this thesis is that the rheological properties of different formulations are noticeably changed by the protein content as well as the protein source.

## **1.2 Objectives**

Throughout this thesis, the following specific objectives were addressed:

- To model the viscosity of ice-cream mixes as a function of protein content, protein source, and temperature (Chapter 2).
- To determine the mechanical spectra of ice-cream mixes as a function of protein content, protein source, and temperature (Chapter 2).

- To model the creep-recovery behavior of ice-cream mixes as a function of protein content, protein source, and temperature (Chapter 3).

### 1.3 References

- Ferry, J. D. (1980). *Viscoelastic properties of polymers*: John Wiley & Sons.
- Hazlett, R., Schmidmeier, C., & O'Mahony, J. A. (2021). Approaches for improving the flowability of high-protein dairy powders post spray drying – A review. *Powder Technology*, 388, 26-40.
- Jana, A. (2022). Chapter 8 - High protein dairy foods: technological considerations. In A. G. d. Cruz, C. S. Ranadheera, F. Nazzaro, & A. M. Mortazavian (Eds.), *Dairy Foods* (pp. 159-193): Woodhead Publishing.
- McGregor, R. A., & Poppitt, S. D. (2013). Milk protein for improved metabolic health: a review of the evidence. *Nutrition & Metabolism*, 10(1), 1-13.
- Steffe, J.F. (1996). *Rheological Methods in Food Process Engineering*, second ed. Freeman Press, East Lansing, MI, USA.
- Tang, M., O'Connor, L. E., & Campbell, W. W. (2014). Diet-Induced weight loss: the effect of dietary protein on bone. *Journal of the Academy of Nutrition and Dietetics*, 114(1), 72-85.
- Thomas, E., Karsten, B., Sahin, F. N., Ertetik, G., Martines, F., Leonardi, V., Paoli, A., Gentil, P., Palma, A., & Bianco, A. (2019). Protein supplement consumption is linked to time spent exercising and high-protein content foods: A multicentric observational study. *Heliyon*, 5(4), e01508.



## Chapter 2

### Modeling the viscosity of ice-cream mixes<sup>1</sup>

#### 2.1 Introduction

A deficit in the quality and quantity of dietary protein disrupts energy regulation, leading to increase food intake and weight gain (Gehring, Gaudichon, & Even, 2020). Nowadays, proteins are considered as an important part of a healthy diet, and an effective strategy to promote weight loss (Tang, O'Connor, & Campbell, 2014). Indeed, a daily protein intake of 1.2 to 2.0 g per kg of body weight per day is recommended for increasing lean body mass (Thomas et al., 2019). Furthermore, proteins from different sources (e.g., vegetable, beef, and dairy) are used to formulate a number of products, such as beverages, snacks, desserts, dietary supplements, and weight-loss products.

Concentrate and isolates of milk proteins are notable for their nutritional (e.g., amino acid profile) and technological (e.g., foaming and emulsification) properties (Hazlett, Schmidmeier, & O'Mahony, 2021). Powdered milk proteins, such as whey protein concentrate (WPC) and milk protein concentrate (MPC) are commonly used to increase the dietary protein in many novelty foods (Hammam, Martinez-Monteagudo, & Metzger, 2021). Technological considerations for increasing the amount of milk proteins in food products can be found elsewhere (Jana, 2022). An attractive novelty food with increased dietary protein is high-protein ice-cream, where the amount of protein is increased up to 8-fold compared with regular ice-cream (1-2 g of protein). The global market for ice-cream is expected to grow from about \$70 billion in 2020 to about \$96 billion by 2028 (Fior

---

<sup>1</sup> A version of this chapter has been submitted for publication in *Journal of Food Processing Engineering*

Markets, 2021). It is likely that the number of consumers attracted to frozen desserts containing protein will increase as well.

The increment of about 6-8-fold of protein in the formulation significantly alters the flow characteristics of the ice-cream mix, which in turn, impacts a number of quality parameters of the resulting ice-cream. Overall, a more viscous ice-cream mix influences the number and size of ice crystals, the residence time, the extent of fat destabilization, the percentage of overrun, and the development of microstructure (Bolliger, Wildmoser, Goff, & Tharp, 2000; Freire, Wu, & Hartel, 2020; Douglas Goff, 2002; Wu, Freire, & Hartel, 2019). Despite the technological relevance, there is a paucity of studies on the influence of protein content on the flow characteristics of ice-cream mix. Daw and Hartel (2015) reported faster melt rates in ice cream with increased protein content (4-10%) due to the increased viscosity within the mix. Similarly, faster melting rates were reported in ice-cream containing whey protein concentrate (8% total protein) when compared with regular ice-cream (Moschopoulou, Dernikos, & Zoidou, 2021). Patel, Baer, and Acharya (2006) also reported higher viscosity in ice-cream with increased protein (up to 7%) with MPC and reported a shrinkage defect due to a collapse of the air cell. Roy, Hussain, Prasad, and Khetra (2021) used whey protein isolate to increase the protein content (10%) in ice-cream and reported higher melting rates compared with the regular ice-cream.

In summary, research in high-protein ice-cream has been focused on the impact of protein source and concentration on the resulting quality of ice-cream (e.g., sensory attributes, melt rates, and hardness). This work reports the rheological characteristics of

ice-cream mix formulated with MPC80 and WPC80. The objective of this chapter is to model the viscosity of ice-cream mixes as a function of protein content (4-12%) and temperature (5-35°C); and (2) to study the mechanical spectra.

## **2.2 Materials and methods**

### **2.2.1 Formulations**

The impact of the protein content (4, 10, and 12%) as well as the protein source (MPC80 and WPC80) was evaluated on the rheological behavior of ice-cream mixes. Ice-cream mixes were formulated according to the guidelines reported elsewhere (Sim, Enteshari, Rathnakumar, & Martínez-Monteaudo, 2021). The ice-cream mixes consisted of 4-12% of total protein, 12-4% of total fat, 25% of total carbohydrates, and 0.3% of a blend of stabilizers. Firstly, a predetermined amount of either milk protein concentrate 80 (Milk specialties, Eden Prairie, MN, USA) or whey protein concentrate 80 (Milk specialties) was dissolved in distilled water for 40 min at 60°C under constant stirring. In a separate container, the carbohydrate blend comprising of 3.9% of lactose monohydrate ( $\geq 98\%$ , Sigma-Aldrich, St. Louis, MO, USA), 14% of granulated sugar (United Sugar Corp., Minneapolis, MN, USA), and 4.0% of dry corn syrup (Cerestar USA, Inc., Hammond, IN, USA) was dissolved in distilled water for 20 min at 55°C under constant stirring. Then, both solutions (protein and carbohydrates) were mixed, and the fat content was adjusted with commercial heavy cream (Great Value™ Walmart, Brookings, SD, USA). Then, the stabilizers were added into the solution and stirred for an additional 10 min at 55°C. The blend of stabilizers (Continental Colloids, Inc., West Chicago, IL, USA) consisted of guar gum, locust bean gum, carrageenan, polysorbate 80, and mono- and

diglycerides. Finally, the mixes were blended with a kitchen blender (Thermomix® TM6™, Vorwerk, Wuppertal, Germany). The total solids for all ice-cream mixes were about 40%, and the pH was about 6.4.

### 2.2.2 Rheological measurements

The rheological behavior of the ice-cream mixes was determined with an MCR90 rheometer (Anton Paar, GmbH, Ostfildern, Germany) equipped with a parallel-plate configuration (a plate diameter of 25 mm and a gap size of 0.14 mm). The mixes were tested at 5, 15, 25, and 35°C using two types of tests – flow curve (flow behavior for low and high shear rates) and frequency sweeps (rate of deformation of the sample). Flow curves of ice-cream mixes were determined within a shear rate range of 1-100/s, recording a total of 25 data points per test. Details of the methodology can be found elsewhere (Sim et al., 2021). Frequency sweep measurements were determined at 0.2 Pa over a frequency range from 0.1 to 10 Hz, according to the methodology reported elsewhere (Martínez-Monteagudo et al., 2017).

### 2.2.3 Data analysis

#### *Modeling the flow behavior*

The viscosity ( $\eta$ ) of the different ice-cream mixes as a function of the shear rate ( $\dot{\gamma}$ ) was represented with the Herschel-Bulkley model, a generalized model of non-Newtonian fluid (Equation (1)):

$$\eta = \eta_o + m_{(T,p)} \cdot \dot{\gamma}^{(n-1)} \quad (\text{Equation 1})$$

where  $\eta_o$  is the yield stress (Pa);  $m_{(T,p)}$  is the consistency index (Pa s<sup>n</sup>) influenced by the temperature and protein content; and  $n$  is the flow behavior index. The temperature and protein dependence on the consistency index ( $m_{(T,p)}$ ) was independently quantified according to Equation (2) and Equation (3), respectively:

$$m_T = m_{T_o} + \exp(-a_T \cdot (T - T_r)) \quad (\text{Equation 2})$$

$$m_p = m_{p_o} + \exp(a_p \cdot (p - p_r)) \quad (\text{Equation 3})$$

where  $m_T$  and  $m_p$  are the temperature and protein dependence on the consistency index;  $a_T$  and  $a_p$  are the sensitivity parameter for temperature and protein, respectively;  $T$  is the temperature (°C);  $p$  is the protein content (%);  $m_{T_o}$  and  $m_{p_o}$  are regression parameters. The average values of the experimental temperature and protein content were used as the  $T_r$  and  $p_r$ , respectively.

Prior to the prediction of viscosity values, the accuracy of the parameters corresponding to the temperature ( $m_{T_o}$  and  $a_T$ ) and protein dependence ( $m_{p_o}$  and  $a_p$ ) was evaluated through joint confidence interval (90%), as recommended elsewhere (Martínez-Monteagudo & Saldaña, 2015). Afterward, the influence of the temperature and protein content was computed using Equation (2.4), which was further incorporated into Equation (1) to yield Equation (5).

$$m_{(T,p)} = m_{T_o} \cdot \exp^{-a_T \cdot (T-T_r)} \cdot \exp^{a_p \cdot (p-p_r)} \quad (\text{Equation 4})$$

$$\eta = \eta_o + [m_{T_o} \cdot \exp^{-a_T \cdot (T-T_r)} \cdot \exp^{a_p \cdot (p-p_r)}] \cdot \dot{\gamma}^{(n-1)} \quad (\text{Equation 5})$$

The viscosity for each experimental temperature and protein content ( $\eta_{exp}$ ) within a shear rate range of 1 to 100 1/s was compared with the predicted viscosity ( $\eta_{pred}$ ) obtained with Equation (5). The parameters of Equation (1) to (5) were calculated through non-linear regression analysis using Athena Visual Workbench ([www.athenavisual.com](http://www.athenavisual.com)). The predictive capability of the model was assessed by the coefficient of determination ( $R^2$ ), the adjusted coefficient of determination ( $R_{Adj}^2$ ), and average absolute percentage of residuals ( $E$ ). All figures were made using Sigma plot software V14.5 for Windows (SPSS Inc., Chicago, IL, USA).

### ***Frequency sweep analysis***

The complex shear module ( $G^*$ ) was computed with the rheometer software, while the storage module ( $G'$ ) and the loss module ( $G''$ ) were calculated using the phase angle ( $\delta$ ), according to Equation (6) and Equation (7):

$$G' = G^* \cdot \cos (\delta) \quad (\text{Equation 6})$$

$$G'' = G^* \cdot \sin (\delta) \quad (\text{Equation 7})$$

Changes in the viscoelastic properties of the ice-cream mixes, in terms of complex module  $G_{(\omega)}^*$ , due to the temperature and protein content were evaluated through a power-law model (Equation (8)) as reported elsewhere (Ferry, 1980).

$$G'_{(\omega)} = A \cdot \omega^b \quad (\text{Equation 8})$$

Where  $A$  is the gel strength ( $\text{Pa s}^{1/z}$ );  $\omega$  is the frequency (Hz); and  $b$  is a dimensionless parameter.

## 2.3 Results and discussion

### 2.3.1 Flow curves

The effect of the protein source (MPC80 and WPC80), protein concentration (4, 8, and 12%), and temperature (5, 10, 15, 25, and 35°C) on the viscosity of ICM is illustrated in a logarithmic graph, **Figure 1**. Overall, the viscosity of all mixes decreased with increasing the shear rate, exhibiting a shear-thinning behavior. This type of behavior has been reported in regular (Sim et al., 2021), high protein (Daw & Hartel, 2015), and low-fat ice-cream mixes (Liu, Wang, Liu, Wu, & Zhang, 2018). Ice-cream mixes are colloidal systems in nature (Goff, 1997), where fat droplets emulsified by proteins, are aggregated, and dispersed in a continuous phase, and an increase in the shear rate disrupts the aggregates, thus reducing their size and viscosity (Rossa, Burin, & Bordignon-Luiz, 2012).

### *Fitting primary models*

The Herschel-Bulkley model (Equation (1)) satisfactorily represented the viscosity values for all mixes. This model has been used to represent the viscosity of ICM containing soy proteins and hydrolysates (Chen et al., 2019), and quince seed (Kurt & Atalar, 2018). In this work, the consistency index was parametrized in a form of exponential model that accounts for the effect of temperature and protein content (Equation (2) and (3), respectively). The opposing in the sensitivity factor ( $a_T$  and  $a_p$ ) reflects the decreasing effect of temperature and increasing effect of protein content. A graphical representation of such dependencies for ICM formulated with MPC80 and WPC80 is given in **Figure 2**.



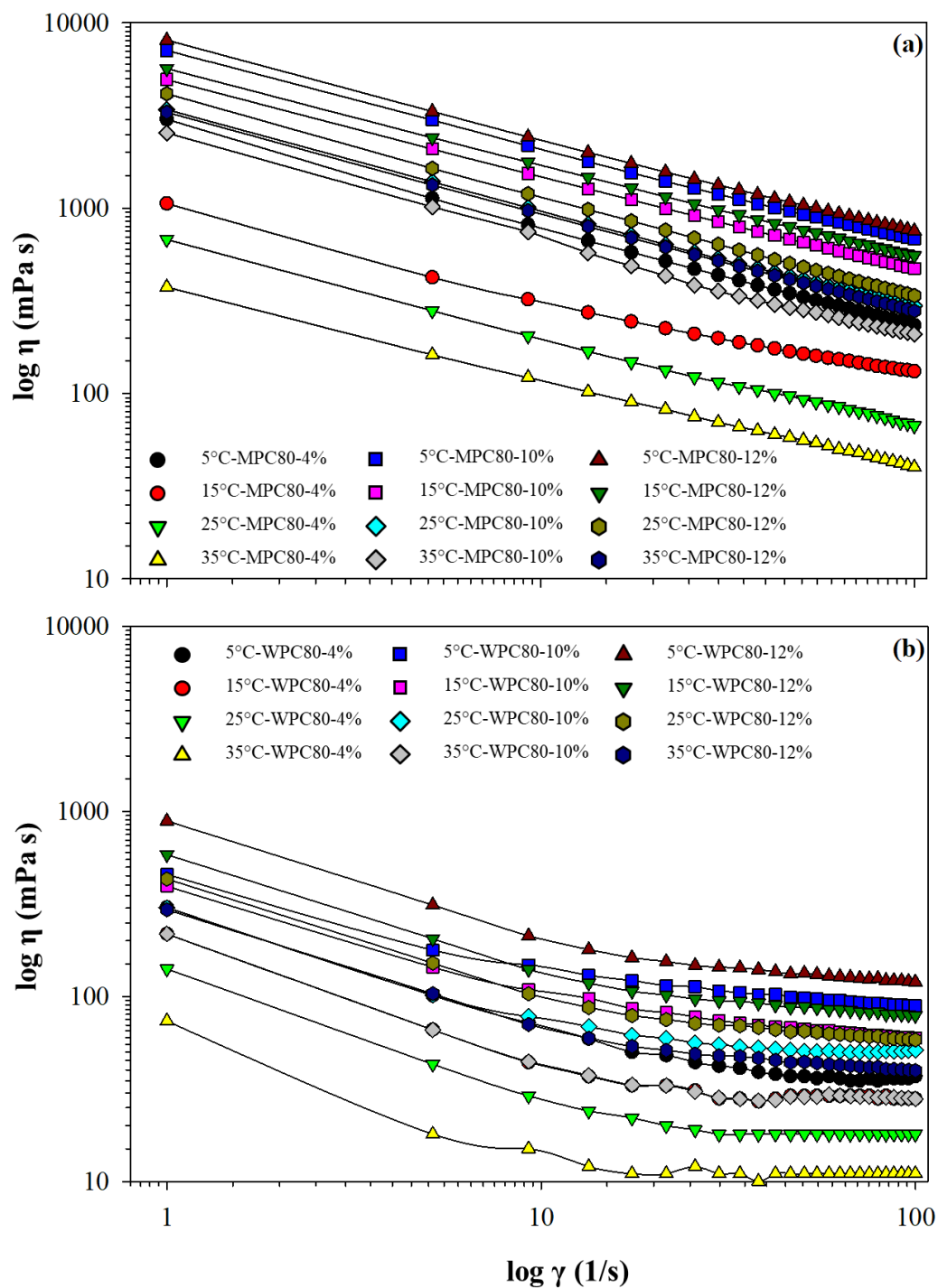


**Figure 1.** Effect of temperature (5, 15, 25, and 35°C) and protein content (4, 10, and 12%) on the logarithmic flow curve of ice-cream mixes: (a) milk protein concentrate 80 (MPC80) and (b) whey protein concentrate 80 (WPC80).

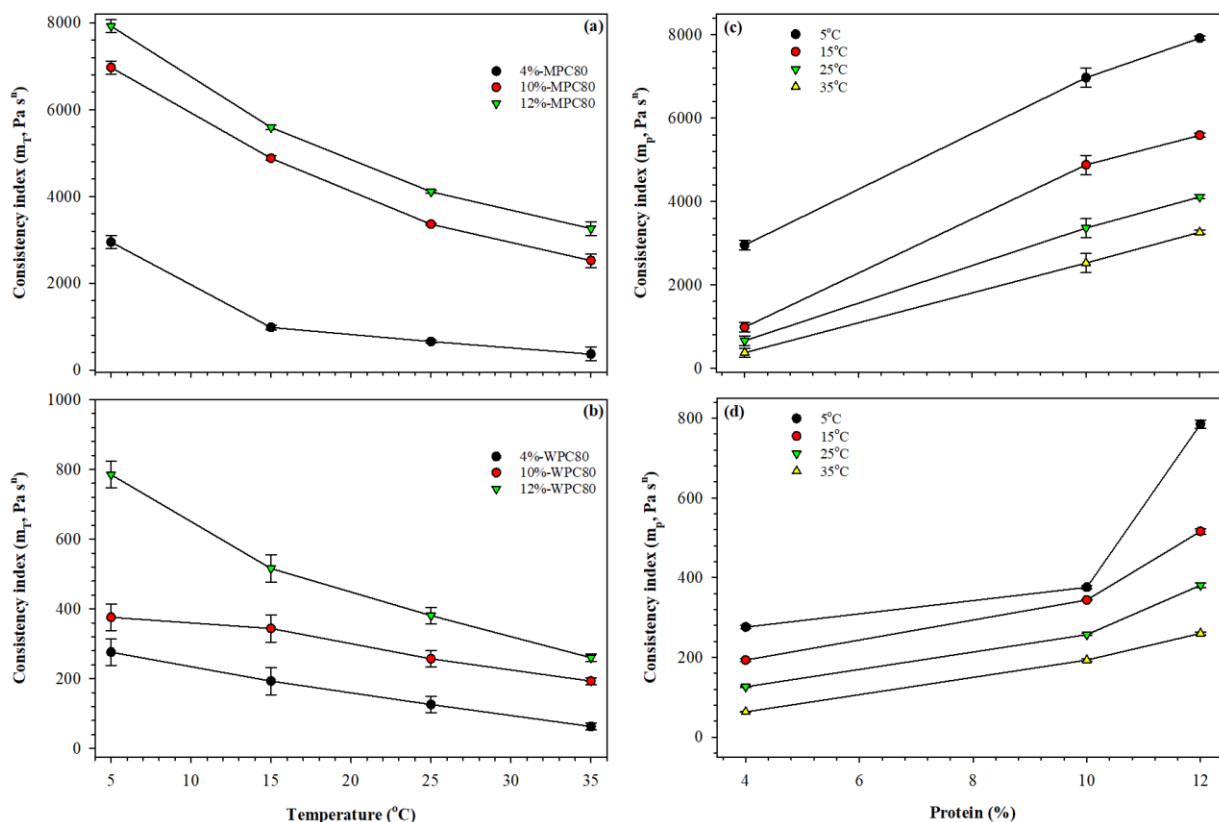


**Figure 2.** Effect of temperature and protein on the consistency index ( $m_T$  and  $m_p$ , respectively) of ice-cream mixes containing different protein content: (a) milk protein concentrate 80 (MPC80) and (b) whey protein concentrate 80 (WPC80).

At a protein content of 12% with MPC80 (**Figure 2a**), the consistency index gradually decreased with the temperature from about 7,900 to 3,200 Pa s<sup>n</sup> at 5 and 35°C, respectively. Similar behavior of lesser magnitude was observed at a protein content of 10 and 4% with MPC80. Daw and Hartel (2015) reported values of consistency index for ICM containing 10% protein within the range of 3,000-8,000 Pa s<sup>n</sup>, depending on the protein source. For ICM formulated with WPC80 (**Figure 2b**), the consistency index values were approximately 10-fold less compared with ICM formulated with MPC80. On the other

hand, the consistency index values gradually increased with the protein content (**Figure 2c** and **2d**). Overall, ICM with MPC80 resulted in higher values of consistency index compared with ICM with WPC80, regardless of the concentration. In MPC80, the native casein: whey protein ratio (80:20) is maintained (Jana, 2022), while the proteins in WPC80 are mostly whey proteins. Casein micelles are much larger than whey proteins, resulting in higher viscosity at the same protein content.

The fitting parameters of the Herschel-Bulkley model are displayed in **Table 1**. All the ice-cream mixes were satisfactorily modeled by the Herschel-Bulkley model, yielding  $R^2$  values higher than 0.997. The temperature and protein dependency on the consistency index decreased with the temperature and decreased with the protein content. Interestingly, the flow behavior index narrowly varied from 0.38 to 0.44 and 0.13 to 0.21 for MPC80 and WPC80, respectively. The flow behavior index was not statistically different between the temperatures and slightly different with respect to the protein content. A true temperature and protein dependence of the flow behavior index can be determined by adding more experimental data points.

### *Fitting secondary models*

Although Equation (2) and (3) account for the temperature and protein effects, respectively, the correlation between the adjustable parameters ( $m_{T0}$ ,  $a_T$ ,  $m_{p0}$ , and  $a_p$ ) cannot be ignored. Thus, the 90% joint confidence region was determined (**Figure 3**) as a mean to evaluate the relationship between the adjustable parameters –  $a_T$  vs  $m_{T0}$  and  $a_p$  vs  $m_{p0}$ .

**Table 1.** Parameters of the Herschel-Bulkley model for the ice-cream mixes formulated with different protein content.

Parameters	4%-MPC80			
	5°C	15°C	25°C	35°C
$\eta_o$	66.15 ± 7.61	79.31 ± 3.53	230.30 ± 2.11	9.02 ± 1.26
$m_{(T,p)}$	2952.51 ± 11.59	980.60 ± 5.46	656.05 ± 2.93	366.69 ± 1.58
$n$	0.38 ± 0.01	0.37 ± 0.01	0.42 ± 0.01	0.47 ± 0.01
$R^2$	0.999	0.999	0.999	0.999
Parameters	10%-MPC80			
	5°C	15°C	25°C	35°C
$\eta_o$	128.25 ± 17.83	62.66 ± 2.71	43.85 ± 5.16	31.50 ± 20.94
$m_{(T,p)}$	6972.83 ± 23.52	4881.46 ± 3.47	3364.45 ± 6.97	2524.30 ± 29.87
$n$	0.44 ± 0.01	0.46 ± 0.01	0.43 ± 0.01	0.41 ± 0.01
$R^2$	0.999	0.999	0.999	0.999
Parameters	12%-MPC80			
	5°C	15°C	25°C	35°C
$\eta_o$	160.01 ± 4.19	84.29 ± 3.58	44.38 ± 8.63	32.57 ± 1.95
$m_{(T,p)}$	7917.61 ± 5.64	5587.81 ± 4.59	4105.17 ± 11.81	3263.01 ± 2.61
$n$	0.43 ± 0.01	0.46 ± 0.01	0.42 ± 0.01	0.44 ± 0.01
$R^2$	0.999	0.999	0.999	0.999
Parameters	4%-WPC80			
	5°C	15°C	25°C	35°C
$\eta_o$	27.56 ± 1.68	25.33 ± 1.33	15.67 ± 1.07	10.60 ± 0.27
$m_{(T,p)}$	275.75 ± 3.86	193.01 ± 3.91	125.55 ± 2.41	63.01 ± 1.03
$n$	0.16 ± 0.01	0.24 ± 0.01	0.21 ± 0.01	0.22 ± 0.01
$R^2$	0.999	0.997	0.998	0.998
Parameters	10%-WPC80			
	5°C	15°C	25°C	35°C
$\eta_o$	80.40 ± 1.94	51.05 ± 1.74	45.47 ± 0.94	25.17 ± 1.30
$m_{(T,p)}$	376.42 ± 4.09	343.56 ± 1.57	256.91 ± 2.51	192.73 ± 3.82
$n$	0.21 ± 0.01	0.20 ± 0.01	0.15 ± 0.01	0.19 ± 0.01
$R^2$	0.999	0.999	0.999	0.997
Parameters	12%-WPC80			
	5°C	15°C	25°C	35°C
$\eta_o$	104.65 ± 4.57	68.77 ± 3.01	50.83 ± 2.22	34.65 ± 1.51
$m_{(T,p)}$	785.29 ± 1.09	516.01 ± 7.18	381.42 ± 5.31	260.06 ± 3.62
$n$	0.13 ± 0.01	0.14 ± 0.01	0.13 ± 0.01	0.13 ± 0.01
$R^2$	0.999	0.999	0.999	0.999

MPC80 – milk protein concentrate 80; WPC80 – whey protein concentrate 80;  $\eta_o$  – yield stress (Pa);  $m_{(T,p)}$  – consistency index;  $n$  – flow behavior index;  $R^2$  – coefficient of determination

All the confidence regions exhibited an elliptical shape, suggesting some degree of correlation between the parameters. A rectangular confidence region indicates that there is no correlation between the adjustable parameters (Martínez-Monteagudo & Saldaña, 2015). The confidence region corresponding to the temperature parameters ( $a_T$  and  $m_{T_o}$ ) for MPC80 slightly overlapped between 10 and 12% protein (**Figure 3a**). This behavior indicates that the adjustable parameters are not statistically different between 10 and 12% protein.

In contrast, the confidence region for ICM formulated with WPC80 did not overlap, indicating that their parameters are statistically different, regardless of the protein content (**Figure 3b**). On the other hand, the confidence region corresponding to the protein parameters ( $a_p$  and  $m_{p_o}$ ) for MPC80 and WPC80 showed a squeezed-ellipse shape without overlapping (**Figure 3c and 3d**), an indication that the adjustable parameters are statistically different, and some degree of correlation exists between  $a_p$  and  $m_{p_o}$ . Increasing the number of experimental data points is a strategy to reduce the correlation between parameters (Martínez-Monteagudo & Saldaña, 2014).

### ***Fitting global models***

For each protein source, the dependency of temperature and protein content on the consistency index was combined into an exponential model of the form of Equation (5). The parameters obtained in **Figure 3** were used as initial input in Equation (5) and these parameters were then recalculated by non-linear regression. A summary of the regression analysis is given in **Table 2**.

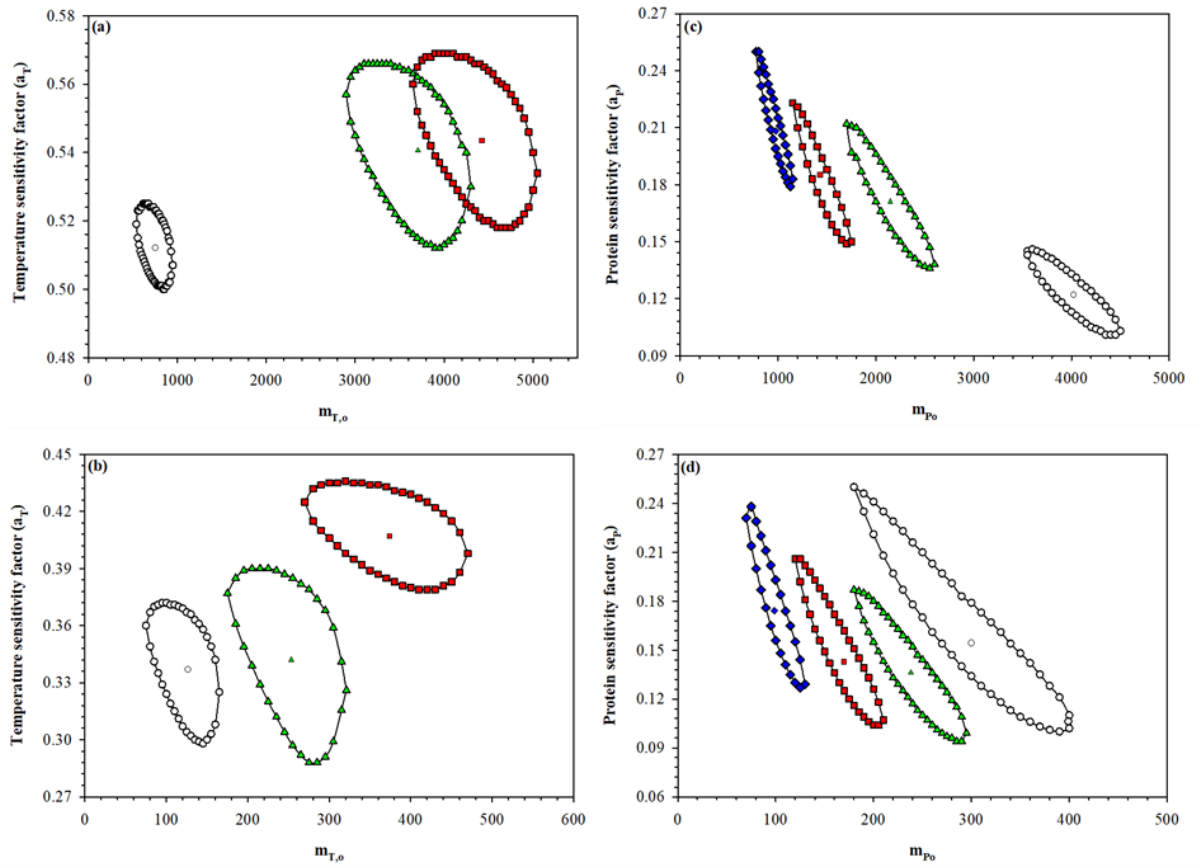


**Figure 3.** Joint confidence region of the regression parameters used to predict the viscosity of ice-cream mixes formulated with different protein content. (a)  $a_T$  vs  $m_{T_o}$  for MPC80 (○ : 4%; ■:10%; and ▲: 12% of protein content), (b)  $a_T$  vs  $m_{T_o}$  for WPC80 (○: 4%; ■:10%; and ▲ : 12% of protein content), (c)  $a_p$  vs  $m_{p_o}$  for MPC80 (○: 5°C; ▲: 15°C;■: 25°C and ◆: 35°C), and (d)  $a_p$  vs  $m_{p_o}$  for WPC80 (○: 5°C;▲: 15°C;■: 25°C and ◆: 35°C).

**Table 2.** Regression analysis of Equation (5) to predict the viscosity as a function of temperature and protein content for ice-cream mixes formulated with milk protein concentrate 80 (MPC80) and whey protein concentrate 80 (WPC80).

Parameter	MPC80	WPC80
	Value $\pm$ 95%CI	Value $\pm$ 95%CI
$\eta_o$	-61.37 $\pm$ 6.32	13.49 $\pm$ 1.66
$m_{T_o}$	2179.17 $\pm$ 101.12	159.46 $\pm$ 14.19
$a_T$	0.034 $\pm$ 0.001	0.037 $\pm$ 0.002
$a_p$	0.141 $\pm$ 0.007	0.173 $\pm$ 0.006
$n$	0.492 $\pm$ 0.013	0.467 $\pm$ 0.021
$R^2$	0.985	0.987
$R^2_{adj}$	0.983	0.982
E	9.72	8.99

MPC80 – milk protein concentrate 80; WPC80 – whey protein concentrate 80;  $\eta_o$  – yield stress;  $m_{T_o}$  – regression parameter of Equation (5);  $a_T$  and  $a_p$  – sensitivity parameter for temperature and protein;  $n$  – flow index;  $R^2$  – coefficient of determination;  $R^2_{Adj}$  – adjusted coefficient of determination; E – average absolute percentage of residuals; 95%CI – 95% confidence interval.

The adjustable parameters in Equation (5) satisfactorily described the viscosity values throughout the entire experimental domain, judging by the  $R^2$  ( $>0.98$ ),  $R^2_{adj}$  ( $>0.98$ ), and E ( $<10\%$ ). A graphical representation of the adjustable parameters in Equation (5) is given in **Figure 4**, where the predicted viscosity is plotted against the experimental data points for both protein sources. All predicted values were linearly correlated with the experimental data and laid within the 95% confidence and prediction band. The linear relation between predicted and experimental points was narrower for WPC80 compared with MPC80, judging by the confidence and prediction bands (**Figure 4b**).

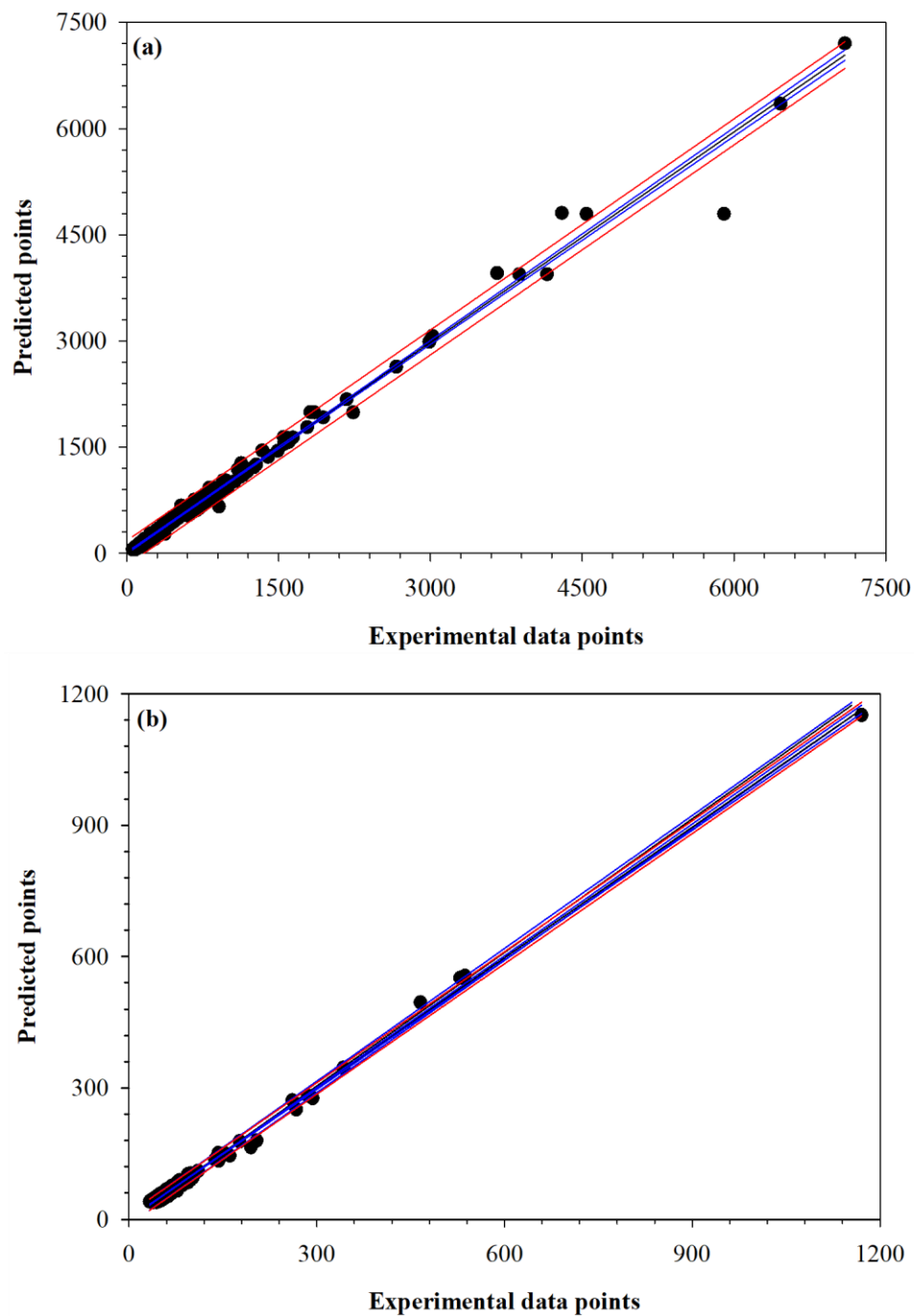


**Figure 4.** Linear relationship between predicted and experimental values of viscosity: (a) milk protein concentrate 80 (MPC80) and (b) whey protein concentrate 80 (WPC80). Blue lines represent the 95% confidence interval band and red lines represent the 95% prediction band.



Values of E lower than 10% are indicative of satisfactory fitting (Martinez-Monteagudo & Salais-Fierro, 2014). The adjustable parameters reported in **Table 2** were used to predict the viscosity of ICM formulated with MPC80 (**Figure 5a**) and WPC80 (**Figure 5b**) within a range of 5-35°C and 4-12% protein content. With this model, the viscosity was predicted at a constant shear rate ( $30 \text{ s}^{-1}$ ). For instance, the viscosity at a constant temperature ( $10^\circ\text{C}$ ) of an ICM containing 8% protein with MPC80 can be obtained by the corresponding contour line.

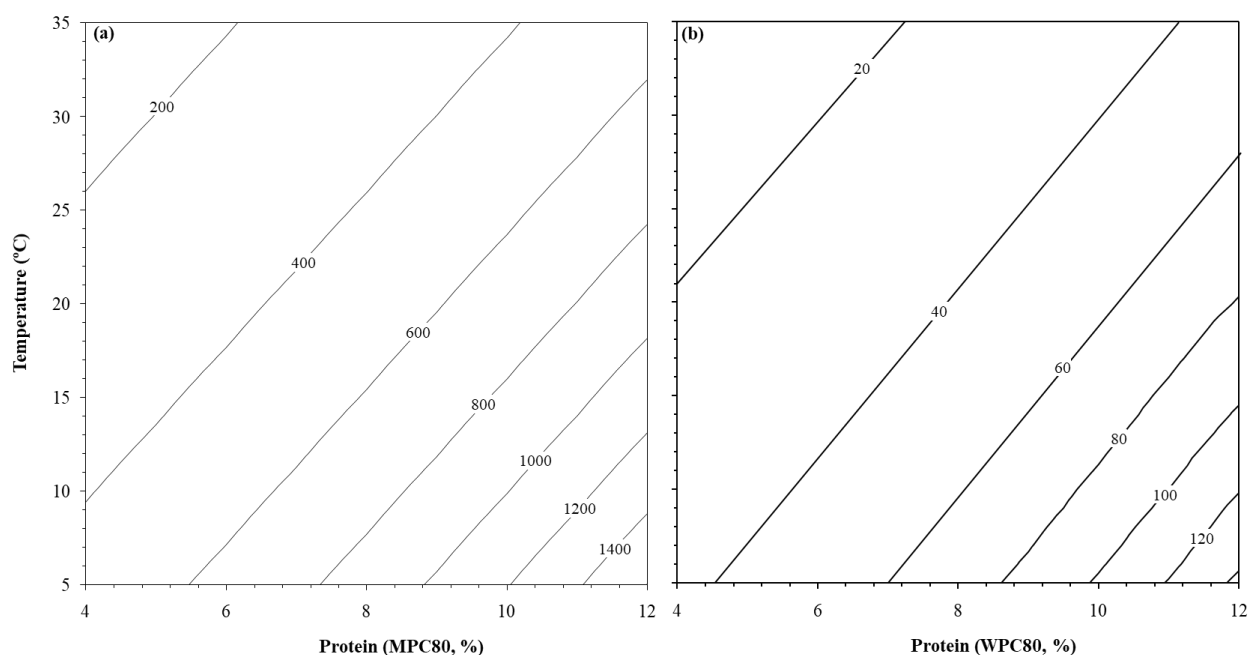


**Figure 5.** Predicted viscosity at as a function of temperature and protein content for ice-cream mixes: (a) milk protein concentrate 80 (MPC80) and (b) whey protein concentrate 80 (WPC80). The viscosity values were predicted with Equation (5) using the estimated parameters (Table 1). Shear rate ( $\dot{\gamma}$ ) was kept constant at  $30 \text{ s}^{-1}$ .

### 2.3.2 Frequency sweeps

The mechanical spectra of ICM measured by frequency sweeps is given in **Figure 6**. For both protein sources,  $G'$  was higher than  $G''$  over the entire frequency range (0.1-10 Hz), exhibiting a viscoelastic liquid behavior and no gel point (Ferry, 1980). Similar mechanical spectra have been reported in regular mix (Sim et al., 2021), low-fat mix (Liu et al., 2018), and mix formulated with quince seed (Kurt & Atalar, 2018). In general,  $G'$  becomes greater than  $G''$  at higher protein content (10-12%), indicating a dominant behavior to form macromolecular networks. Such a behavior has been observed in solutions containing collagen (Oechsle, Häupler, Gibis, Kohlus, & Weiss, 2015), k-carrageenan (Ould Eleya & Turgeon, 2000), and xanthan gum (Mermet-Guyennet et al., 2015).

The weak gel model (Equation (2.8)) was used to obtain information regarding the strength of the gel (**Table 3**). Accordingly, semi-solids foods can be seen as weak structured systems made of a three-dimensional network connected by weak bonds (Domenico Gabriele, de Cindio, & D'Antona, 2001). The relatively large values of  $A$  suggests a dominant viscous gel (Ferry, 1980), and the values increased with the protein content – an indication of stronger elastic structure with increasing the protein content as a result of more intermolecular interactions. Interestingly, no particular trend was observed with respect to the temperature (**Table 2.3**). Similar values of  $A$  has been reported in yogurt (Domenico Gabriele et al., 2001) and dairy emulsions (Gabriele et al., 2011). On the other hand, the ICM formulated with MPC80 and WPC80 were stable, judging by moderate increased of the parameter  $b$  with the temperature (**Table 3**). Moreover, all ICM yielded values of parameter  $b$  were  $<1.0$ , exhibiting characteristics of viscous gel.

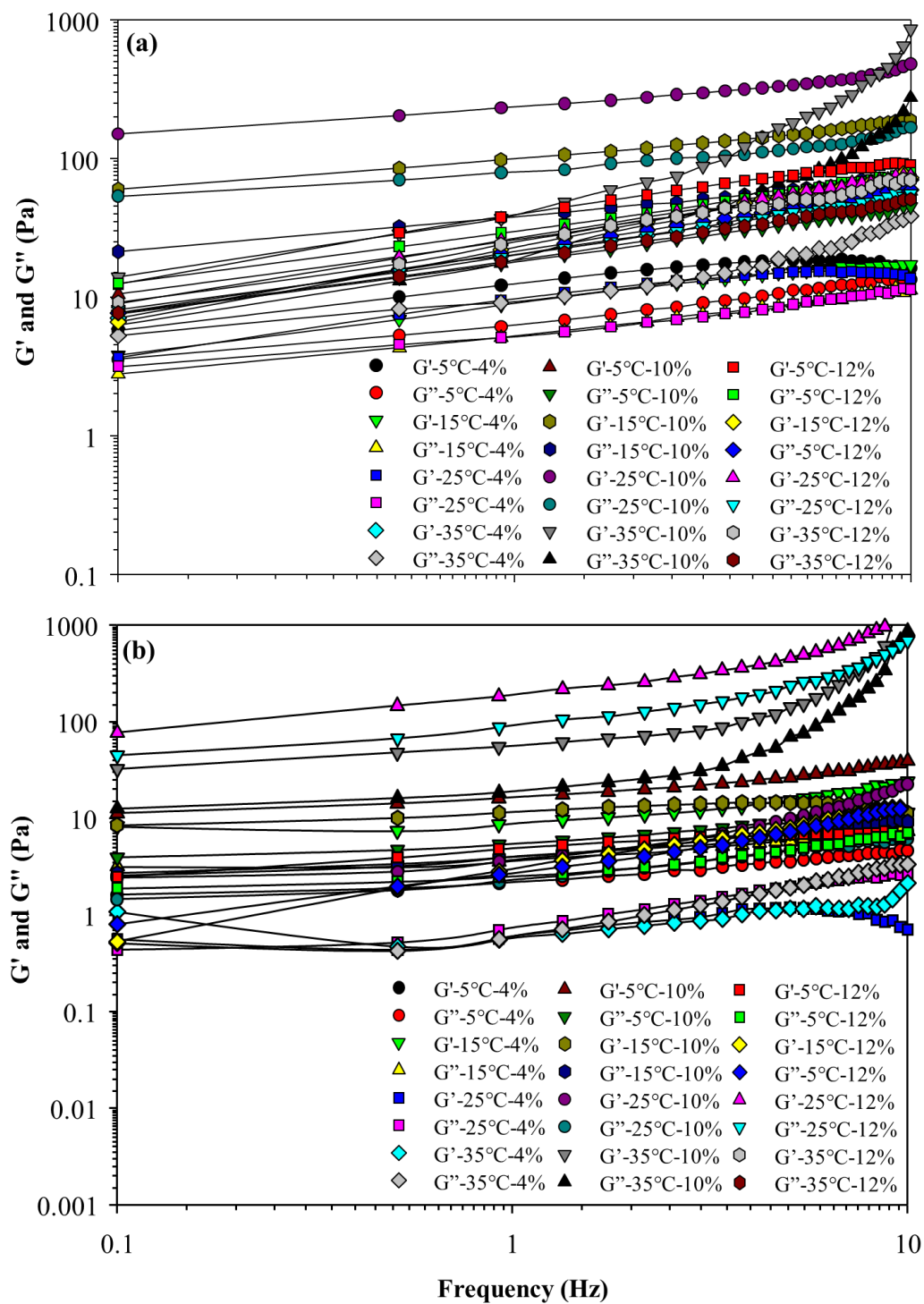


**Figure 6.** Frequency sweep analysis of ice-cream mixes formulated containing different protein content: (a) milk protein concentrate 80 (MPC80) and (b) whey protein concentrate 80 (WPC80).

**Table 3.** Relationship between storage module ( $G'$ ) and frequency ( $\omega$ ) for the ice-cream mixes formulated with different protein content.

Parameters	4%-MPC80			
	5°C	15°C	25°C	35°C
A	12.91 ± 1.03	9.21 ± 0.33	9.96 ± 0.71	18.28 ± 1.16
b	0.18 ± 0.04	0.29 ± 0.02	0.22 ± 0.04	0.54 ± 0.03
R <sup>2</sup>	0.918	0.985	0.921	0.989
Parameters	10%-MPC80			
	5°C	15°C	25°C	35°C
A	26.64 ± 0.67	97.55 ± 2.7	129.09 ± 9.13	124.58 ± 4.70
b	0.36 ± 0.01	0.27 ± 0.02	0.25 ± 0.02	0.64 ± 0.16
R <sup>2</sup>	0.995	0.988	0.973	0.981
Parameters	12%-MPC80			
	5°C	15°C	25°C	35°C
A	40.14 ± 1.31	24.08 ± 0.83	26.17 ± 0.68	24.32 ± 1.62
b	0.38 ± 0.02	0.49 ± 0.02	0.46 ± 0.01	0.47 ± 0.03
R <sup>2</sup>	0.993	0.996	0.997	0.981
Parameters	4%-WPC80			
	5°C	15°C	25°C	35°C
A	4.07 ± 0.09	8.34 ± 1.08	7.46 ± 1.01	7.89 ± 1.31
b	0.25 ± 0.01	0.41 ± 0.07	0.18 ± 0.08	0.24 ± 0.05
R <sup>2</sup>	0.997	0.904	0.921	0.902
Parameters	10%-WPC80			
	5°C	15°C	25°C	35°C
A	15.68 ± 1.19	12.03 ± 1.26	10.55 ± 0.43	11.82 ± 0.75
b	0.35 ± 0.04	0.46 ± 0.08	0.55 ± 0.09	0.39 ± 0.07
R <sup>2</sup>	0.955	0.923	0.974	0.898
Parameters	12%-WPC80			
	5°C	15°C	25°C	35°C
A	15.68 ± 1.19	12.03 ± 0.82	23.15 ± 0.43	14.68 ± 0.75
b	0.35 ± 0.04	0.46 ± 0.04	0.47 ± 0.06	0.39 ± 0.08
R <sup>2</sup>	0.955	0.942	0.977	0.892

A and z – regression parameters of Equation (8); R<sup>2</sup> coefficient of determination; MPC80 – milk protein concentrate 80; WPC80 – whey protein concentrate 80. The error bars were obtained through the 95% confidence interval.

## 2.4 Conclusions

The rheological properties of the ICM were significantly influenced by the protein source, protein content, and temperature. The viscosity of the ice-cream mixes was modeled using the Herschel-Bulkley model, where the consistency index was parametrized to account for the effect of temperature and protein content. The mechanical spectra of the ICM suggested a stronger elastic structure with increasing the protein content.

## 2.5 References

- Bolliger, S., Wildmoser, H., Goff, H. D., & Tharp, B. W. (2000). Relationships between ice cream mix viscoelasticity and ice crystal growth in ice cream. *International Dairy Journal*, 10(11), 791-797.
- Chen, W., Liang, G., Li, X., He, Z., Zeng, M., Gao, D., Qin, F., Goff, H.D., Chen, J. (2019). Effects of soy proteins and hydrolysates on fat globule coalescence and meltdown properties of ice cream. *Food Hydrocolloids*, 94, 279-286.
- Daw, E., & Hartel, R. W. (2015). Fat destabilization and melt-down of ice creams with increased protein content. *International Dairy Journal*, 43, 33-41.
- Ferry, J. D. (1980). *Viscoelastic properties of polymers*: John Wiley & Sons.
- Fior Markets (2021). *Global Ice Cream Market*. Retrieved from mordorintelligence.com.
- Freire, D. O., Wu, B., & Hartel, R. W. (2020). Effects of structural attributes on the rheological properties of ice cream and melted ice cream. *Journal of Food Science*, 85(11), 3885-3898.
- Gabriele, D., de Cindio, B., & D'Antona, P. (2001). A weak gel model for foods. *Rheologica Acta*, 40(2), 120-127.

- Gabriele, D., Migliori, M., Baldino, N., Di Sanzo, R., de Cindio, B., & Vuozzo, D. (2011). Rheological characterisation of dairy emulsions for cold foam applications. *International Journal of Food Properties*, *14*, 786–798.
- Gehring, J., Gaudichon, C., & Even, P. C. (2020). Food intake control and body weight regulation by dietary protein. *Cahiers de Nutrition et de Di t tique*, *55*(6), e1-e8.
- Goff, H. D. (1997). Colloidal aspects of ice cream—A review. *International Dairy Journal*, *7*(6-7), 363-373.
- Goff, H. D. (2002). Formation and stabilisation of structure in ice-cream and related products. *Current Opinion in Colloid & Interface Science*, *7*(5), 432-437.
- Hammam, R. A., Martinez-Monteagudo, S. I., & Metzger, L. E. (2021). Progress in micellar casein concentrate: Production and applications. *Comprehensive Reviews in Food Science and Food Safety*, *20*(5), 4426-4449.
- Hazlett, R., Schmidmeier, C., & O'Mahony, J. A. (2021). Approaches for improving the flowability of high-protein dairy powders post spray drying – A review. *Powder Technology*, *388*, 26-40.
- Jana, A. (2022). Chapter 8 - High protein dairy foods: technological considerations. In A. G. d. Cruz, C. S. Ranadheera, F. Nazzaro, & A. M. Mortazavian (Eds.), *Dairy Foods* (pp. 159-193): Woodhead Publishing.
- Liu, R., Wang, L., Liu, Y., Wu, T., & Zhang, M. (2018). Fabricating soy protein hydrolysate/xanthan gum as fat replacer in ice cream by combined enzymatic and heat-shearing treatment. *Food Hydrocolloids*, *81*, 39-47.
- Mart nez-Monteagudo, S. I., Kamat, S., Patel, N., Konuklar, G., Rangavajla, N., & Balasubramaniam, V. M. (2017). Improvements in emulsion stability of dairy

beverages treated by high pressure homogenization: A pilot-scale feasibility study. *Journal of Food Engineering*, 193, 42-52.

Martinez-Monteagudo, S. I., & Salais-Fierro, F. (2014). Moisture sorption isotherms and thermodynamic properties of mexican mennonite-style cheese. *Journal of Food Science and Technology*, 51(10), 2393-2403.

Martínez-Monteagudo, S. I., & Saldaña, M. D. A. (2014). Modeling the retention kinetics of conjugated linoleic acid during high-pressure sterilization of milk. *Food Research International*, 62, 169-176.

Martínez-Monteagudo, S. I., & Saldaña, M. D. A. (2015). Retention of bioactive lipids in heated milk: Experimental and modelling. *Food and Bioproducts Processing*, 94, 290-296.

Mermet-Guyennet, M. R. B., Castro, J. G. d., Habibi, M., Martzel, N., Denn, M. M., & Bonn, D. (2015). LAOS: The strain softening/strain hardening paradox. *Journal of Rheology*, 59(1), 21-32.

Moschopoulou, E., Dernikos, D., & Zoidou, E. (2021). Ovine ice cream made with addition of whey protein concentrates of ovine-caprine origin. *International Dairy Journal*, 122, 105146.

Oechsle, A. M., Häupler, M., Gibis, M., Kohlus, R., & Weiss, J. (2015). Modulation of the rheological properties and microstructure of collagen by addition of co-gelling proteins. *Food Hydrocolloids*, 49, 118-126.

Ould Eleya, M. M., & Turgeon, S. L. (2000). Rheology of  $\kappa$ -carrageenan and  $\beta$ -lactoglobulin mixed gels. *Food Hydrocolloids*, 14(1), 29-40.

- Patel, M. R., Baer, R. J., & Acharya, M. R. (2006). Increasing the protein content of ice cream. *Journal of Dairy Science*, *89*(5), 1400-1406.
- Rossa, P. N., Burin, V. M., & Bordignon-Luiz, M. T. (2012). Effect of microbial transglutaminase on functional and rheological properties of ice cream with different fat contents. *LWT - Food Science and Technology*, *48*(2), 224-230.
- Roy, S., Hussain, S. A., Prasad, W. G., & Khetra, Y. (2021). Effect of emulsifier blend on quality attributes and storage of high protein buffalo milk ice cream. *LWT - Food Science and Technology*, *150*, 111903.
- Sim, J. Y., Enteshari, M., Rathnakumar, K., & Martínez-Monteagudo, I. S. (2021). Hydrodynamic cavitation: Process opportunities for ice-cream formulations. *Innovative Food Science & Emerging Technologies*, *70*, 102675.
- Tang, M., O'Connor, L. E., & Campbell, W. W. (2014). Diet-Induced weight loss: the effect of dietary protein on bone. *Journal of the Academy of Nutrition and Dietetics*, *114*(1), 72-85.
- Thomas, E., Karsten, B., Sahin, F. N., Ertetik, G., Martines, F., Leonardi, V., Paoli, A., Gentil, P., Palma, A., & Bianco, A. (2019). Protein supplement consumption is linked to time spent exercising and high-protein content foods: A multicentric observational study. *Heliyon*, *5*(4), e01508.
- Wu, B., Freire, D. O., & Hartel, R. W. (2019). The effect of overrun, fat destabilization, and ice cream mix viscosity on entire meltdown behavior. *Journal of Food Science*, *84*(9), 2562-2571.



## Chapter 3

### Modeling the creep-recovery curves of ice-cream mixes<sup>2</sup>

#### 3.1 Introduction

Ice-cream consists of three distinctive phases (air bubbles, fat globules, and ice crystals) embedded in a concentrated frozen matrix made of proteins and carbohydrates (Eisner, Wildmoser, & Windhab, 2005). This unique material is a result of the interaction between ingredients during the different processing steps. A typical ice-cream is formulated to contain about 8-12% fat, 6-10% non-fat milk solids, 12-16% sweeteners, and <1% minor components, such as flavoring components, emulsifiers, and stabilizers. Overall, the manufacture of ice-cream involves a number of unit operations, including mixing of ingredients, pasteurization, homogenization, aging, freezing, packaging, hardening, and storage. The manufacture of ice-cream is of general knowledge, and specific details on the individual operations can be found elsewhere (Goff, 2015).

Freezing of the ice-cream mix is perhaps the most critical step during the manufacture of ice-cream (Goff, 2015). Prior to freezing, however, the ice-cream mix requires to develop a number of desired physical characteristics, including an optimum particle size distribution, certain degree of fat destabilization, and some flow characteristics. The role of the ingredients and processing step on the development of ice-cream structure can be found elsewhere (Goff, 1997). The homogenization of ice-cream mixes results in a reorganization of the structural elements within a surrounding continuous material (Osorio-Arias, Vega-Castro, & Martínez-Monteagudo, 2020). Thus, homogenized ice-cream mixes

---

<sup>2</sup> A version of this chapter has been submitted for presentation within the XII Ibero-American Congress of Food Engineering, March 15-20, 2022

contain fat droplets of an average size of 0.2 to 0.5  $\mu\text{m}$  distributed within the serum phase (Sim et al., 2021). Moreover, the resulting fat droplets are coated with a layer of protein-emulsifier (Goff, 1997). Air bubbles are produced due to the foaming capacity of protein and fat droplets, while the serum phase consists of sugar and soluble particles.

In summary, ice-cream mixes display characteristics of colloidal solution, and their flow characteristics of the ice-cream mixes has been documented in the literature (Adapa et al., 2000; Toker et al., 2013; Sim et al., 2021). For instance, a typical ice-cream mix exhibits shear thinning behavior, where the viscosity decreased with the shear rate (Regand & Goff, 2003). Another relevant flow characteristic is to determine the viscoelastic linear region and the dominant flow component – viscoelastic solid or viscoelastic liquid (Sim et al., 2021).

The existing literature revealed that ice-cream mixes displayed a dominant behavior of viscoelastic solid (Toker et al., 2013; Kurt, Cengiz, & Kahyaoglu, 2016; Sim et al., 2021). The determination of viscoelasticity of complex systems, such as ice-cream mixes, is carried out through oscillatory tests, yielding the corresponding storage and loss moduli ( $G'$  and  $G''$ , respectively) (Dolz, Hernández, & Delegido, 2008). Additionally, the rheological tests have been related with microscopy techniques to obtain relevant insights on the structural organization of food systems (Brito-Oliveira et al., 2022). Creep-recovery is a different rheological test commonly used to characterize the deformation (creep) and subsequent recovery of complex systems (Huang et al., 2013). Overall, the test of creep-

recovery consists of a creep phase and a recovery phase (Dolz, Hernández, & Delegido, 2008).

In the creep phase, the deformation of a sample subjected to a constant stress for a given time is measured, while the recovery phase measures the ability to recover over a given time after the removal of the stress. Creep-recovery test is performed within the linear viscoelastic region, where the microstructural organization remains intact. In this type of test, the measured response is expressed as the creep compliance ( $J(t)$ ), which is defined as the ration of the measured strain to the applied stress (Brito-Oliveira et al., 2022). A graphical representation of the creep-recovery curves is given in **Figure 7**, where the mechanical models that represents the deformation of the system is illustrated through a dashpot. A typical creep-recovery curve is characterized by an initial elastic response is first detected followed by a delayed elastic response and finally a steady response.

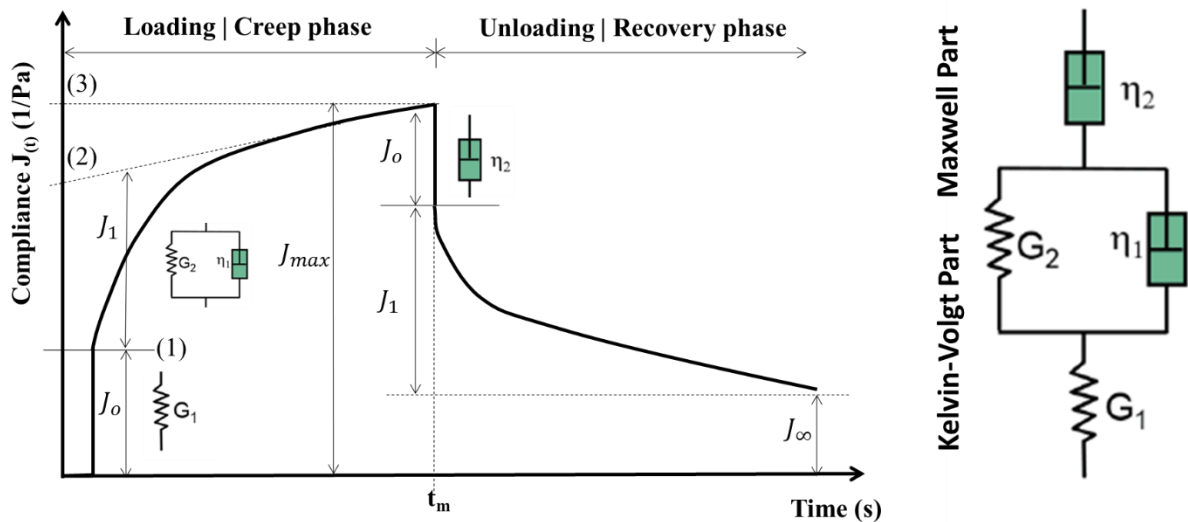


**Figure 7.** Illustration of a typical creep-recovery curve and dashpot of the Burger model consisted of Maxwell and Kelvin-Voigt models in series.

For illustration purpose, the creep phase in **Figure 7** is divided into three main zones, namely instantaneous response, elastic behavior, and viscous flow illustrated by point (1), (2), and (3), respectively (Xu et al., 2008). Point (1) represents the origin of the creep phase to the instantaneous response of the material. Point (2) indicates the beginning of the elastic curve and extends to the viscous flow (point (3)). The elastic behavior of the sample is related to the linkages between the structural units are stretched elastically (Rady, Soliman, & El-Wersh, 2017). Once the stress is removed, the sample will recover to its original structure. The recovery, point (3), is instantaneous and it is made possible by the potential energy of the material.

Creep-recovery curves are commonly described through the Burger model that consisted of four-components. In general, the Burger model comprises the association in series of the Maxwell model and the Kelvin-Voight model. However, the Burger model lacks the capability to simultaneously describe the creep and recovery data. This issue of the Burger model has been highlighted in the literature (Dolz, Hernández, & Delegido, 2008; Toker et al., 2013; Kurt, Cengiz, & Kahyaoglu, 2016; Brito-Oliveira et al., 2022).

The knowledge of the flow properties of the ice-cream mixes provides relevant insights into the mechanical deformation and recovery of the system as well as the impact on the heat and mass transfer. There is, however, a scarcity of studies dealing with the creep-recovery behavior of ice-cream mixes. The objective of this chapter is to model the creep-recovery curves as a function of protein content (4-12%) and temperature (5-35°C).

## 3.2 Materials and methods

### 3.2.1 Formulations

The ice-cream mixes containing different protein content (4, 10, and 12%) were formulated as described in chapter 2 (section 2.3.1).

### 3.2.2 Creep-recovery measurements

The creep-recovery behavior of the ice-cream mixes was determined with an MCR90 rheometer (Anton Paar, GmbH, Ostfildern, Germany) equipped with a parallel-plate configuration (a plate diameter of 25 mm and a gap size of 0.14 mm). The mixes were tested at 5, 15, 25, and 35°C. Creep-recovery measurements were recorded at constant stress amplitude (0.2 Pa) within the linear viscoelastic region, following the methodology reported elsewhere (Kurt, Cengiz, & Kahyaoglu, 2016). The stress was applied and maintained for 150 s, followed by released stress and recovery for an additional 150 s. Each measurement was repeated three times.

The creep-recovery data were expressed using the creep compliance function ( $J(t)$ ), according to Equation (9):

$$J(t) = \frac{\gamma(t)}{\sigma} \quad (\text{Equation 9})$$

where  $\gamma(t)$  is the shear deformation and  $\sigma$  is the applied constant stress. The final recovery of the entire system (% $R$ ) was expressed in percentage, according to Equation (10):

$$\%R = \left[ \frac{J_{Max} - J_{\infty}}{J_{Max}} \right] \cdot 100 \quad (\text{Equation 10})$$

where  $J_{Max}$  is the maximum deformation corresponding to the compliance value once the stress has been removed, and  $J_{\infty}$  is the compliance for the longest time. For each combination of temperature (5, 15, 25, and 35°C) and protein content (4, 10, and 12%), the creep compliance as a function of time was analyzed with the Burger model.

### 3.2.3 Burger model

The Burger model was used to analyze through the four-component that represents the Maxwell and the Kelvin-Voigt model, as illustrated in **Figure 7**. The Burger model in the form of Equation (11) was used to represent the compliance measurements during the creep-recovery curve.

$$J(t) = \begin{cases} J_o + J_1 \cdot \left( 1 - \exp\left(\frac{-t}{\lambda_{ret}}\right) \right) + \frac{t}{\eta_o}; & t \leq t_1 \\ J_1 \cdot \left( \exp\left(\frac{t_1-t}{\lambda_{ret}}\right) - \exp\left(\frac{-t}{\lambda_{ret}}\right) \right) + \frac{t_1}{\eta_o}; & t > t_1 \end{cases} \quad (\text{Equation 11})$$

Where  $J(t)$  is the compliance as a function of time within the creep phase;  $J_o$  is the instantaneous compliance;  $J_1$  is the compliance associated with the Kelvin-Voigt element;  $\lambda_{ret}$  is the retardation time associated with the Kelvin-Voigt element;  $t$  is the test time; and  $\eta_{oM}$  is the viscosity of the Maxwell dashpot; and  $t_1$  is the time when the stressed was removed.

### 3.3 Results and discussion

#### 3.3.1 Creep-recovery curves

**Figure 8** and **Figure 9** show the creep and recovery curves of ICM formulated with MPC80 and WPC80, respectively. The creep phase involves the compliance values over the first 150 s of the curve when a constant shear stress was applied, while the compliance values from 150 to 300 s correspond to the recovery phase after the shear stress was removed.

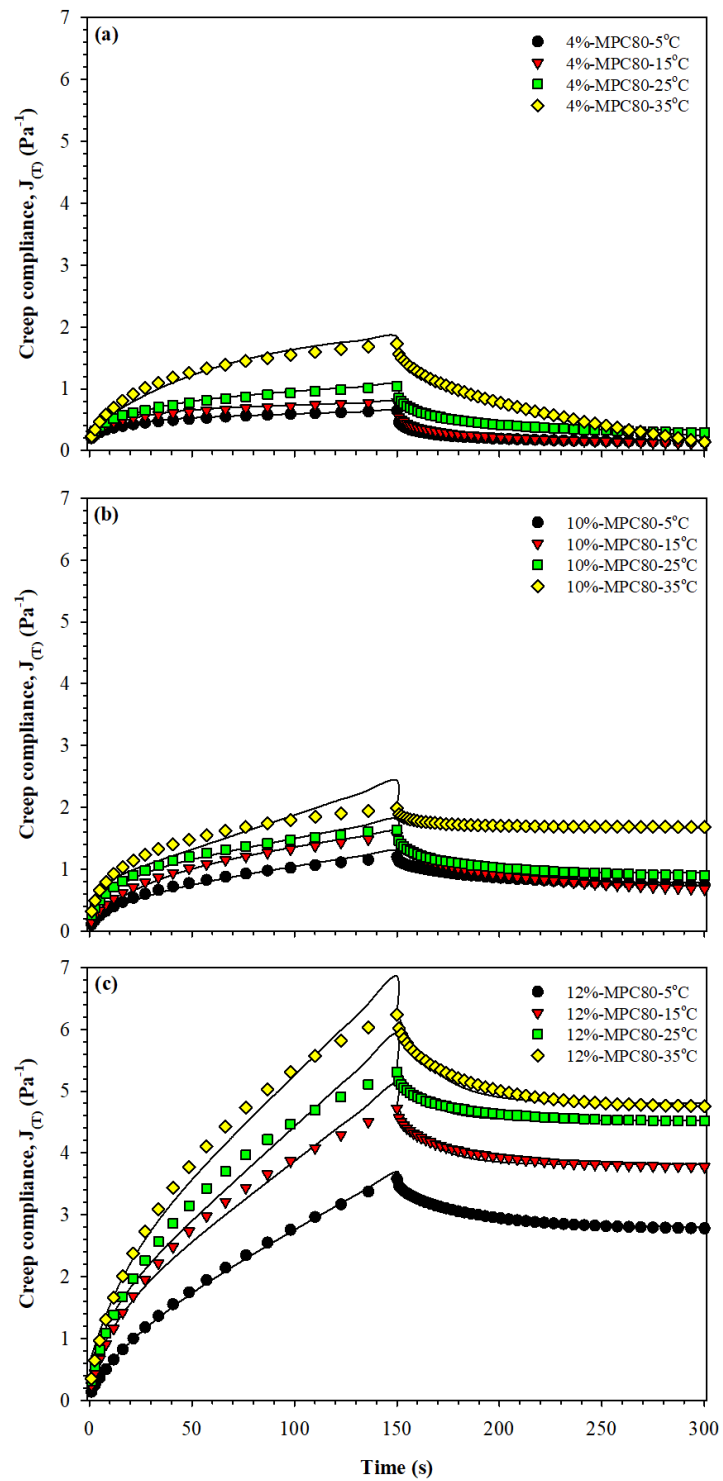


**Figure 8.** Creep-recovery curves of ice-cream mixes formulated with milk protein concentrate 80 (MPC80) at 4, 10, and 12% (a-c). Symbols represents the experimental data while the continuous line represents the Burger model.



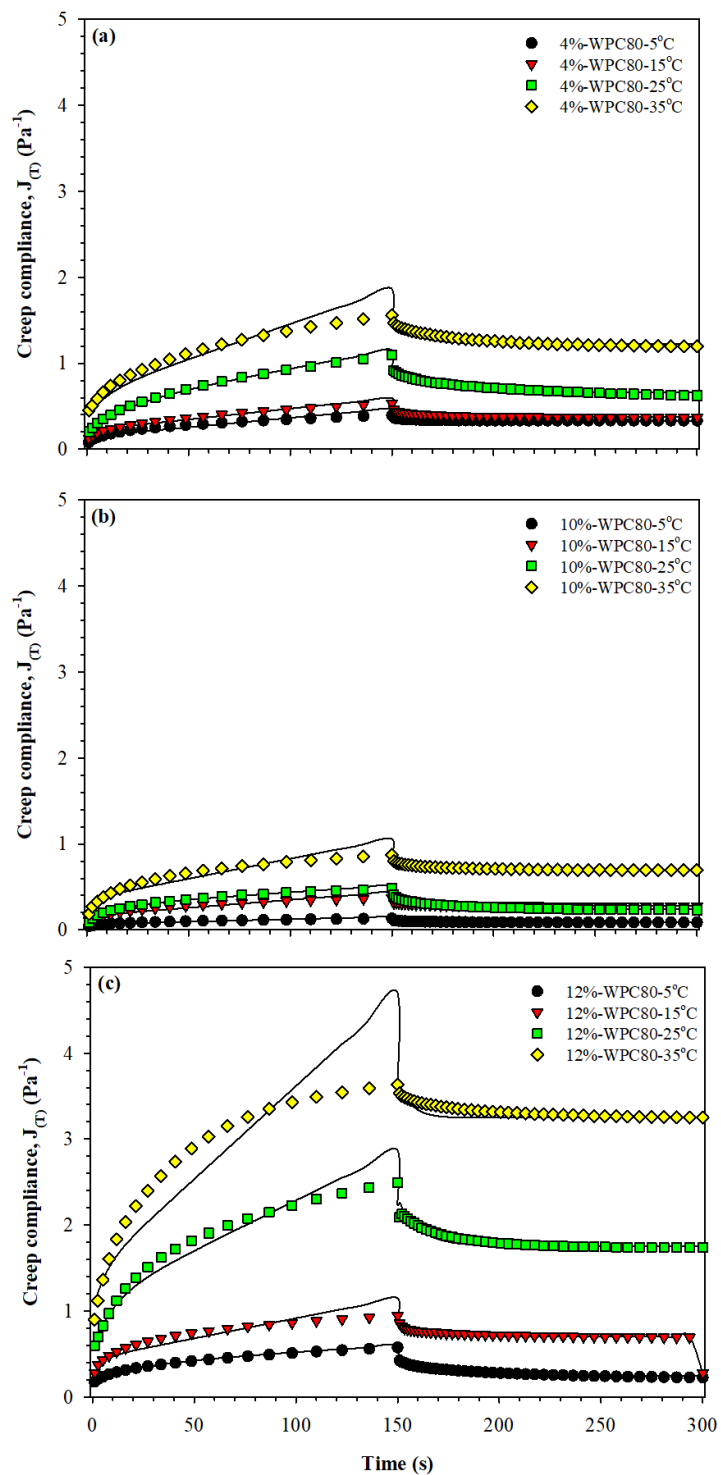


**Figure 9.** Creep-recovery curves of ice-cream mixes formulated with whey protein concentrate 80 (MPC80) at 4, 10, and 12% (a-c). Symbols represents the experimental data while the continuous line represents the Burger model.

All the creep-recovery curves of ICM exhibited a combination of viscous fluid and elastic solid – viscoelastic properties (Onyango et al., 2009). Overall, creep-recovery curves are associated with the reorientation of bonds within the viscoelastic material (Onyango et al., 2009). In the creep phase, an initial elastic deformation (spring of the Maxwell) can be observed followed by gradual deformation (Kelvin-Voigt element) towards an asymptote as time increased.

After the removal of the stress, there was a sharp reduction in compliance due to a residual and irreversible deformation. The compliance values increased with temperature and protein content for both protein sources, being more notorious for MPC80. For instance, the maximum compliance obtained for MPC80 ( $5.89 \text{ Pa}^{-1}$ ) was considerable higher than that for WPC80 ( $3.63 \text{ Pa}^{-1}$ ) when both mixes contained 12% protein and tested at  $35^{\circ}\text{C}$ . Compliance values within the creep phase are generally associated with softness of the material (Sozer, 2009). Materials exhibiting high compliance values had weaker structure than those materials with lower compliance values (Dolz, Hernández, & Delegido, 2008). In MPC80, casein micelles exist in the form of spherical aggregates that add to the voluminous particles in solution (Daw & Hartel, 2015), increasing the colloidal interactions between particles within the mix.

### **3.3.2 Recovery of the system**

The recovery phase started after the removal of the applied stress ( $150 \leq t \leq 300 \text{ s}$ ), where a maximum deformation was obtained. Overall, the  $J_{Max}$  values increased with temperature and protein content for both protein sources. Such an increase in the  $J_{Max}$

values suggest an irreversible breakage of the elastic bonds, causing some degree of structure collapse (Onyango et al., 2009). The ability of ICM to recover its original state was evaluated through Equation (11) (**Table 4**).

**Table 4.** Final percentage recovery for ice-cream mixes formulated with milk protein concentrate 80 (MPC80) and whey protein concentrate 80 (WPC80).

Temperature (°C)	%R – MPC80		
	4%	10%	12%
5	74.49 ± 4.72 <sup>Aa</sup>	37.02 ± 1.85 <sup>Ba</sup>	22.33 ± 2.01 <sup>Ca</sup>
15	80.32 ± 4.01 <sup>Aac</sup>	54.39 ± 2.71 <sup>Bb</sup>	19.12 ± 1.09 <sup>Cb</sup>
25	69.44 ± 3.47 <sup>Ab</sup>	49.82 ± 2.49 <sup>Bc</sup>	23.89 ± 2.21 <sup>Ca</sup>
35	86.97 ± 4.34 <sup>Ac</sup>	15.99 ± 0.89 <sup>Bd</sup>	14.94 ± 1.01 <sup>Bc</sup>
Temperature (°C)	%R – WPC80		
	4%	10%	12%
5	33.61 ± 1.68 <sup>Aa</sup>	16.83 ± 0.83 <sup>Ba</sup>	58.53 ± 2.92 <sup>Ca</sup>
15	25.37 ± 2.26 <sup>Ab</sup>	29.97 ± 2.49 <sup>Ab</sup>	26.77 ± 3.49 <sup>Ab</sup>
25	20.32 ± 1.01 <sup>Ac</sup>	40.85 ± 4.64 <sup>Bc</sup>	10.85 ± 0.83 <sup>Cc</sup>
35	50.32 ± 2.51 <sup>Ad</sup>	22.98 ± 1.14 <sup>Ad</sup>	30.17 ± 1.50 <sup>Cd</sup>

%R – recovery of the entire system; MPC80 – milk protein concentrate 80; WPC80 – whey protein concentrate 80. Mean ± standard deviation (n = 3) within each row with different letters (A–C) is significantly different (P < 0.05) according to Tukey test. Mean ± standard deviation within each column with different letters (a–d) is significantly different (P < 0.05) according to Tukey test.

Temperature, protein content as well as the protein source significantly influenced the %R values. For instance, the highest recovery for MP80 (86.97 ± 4.34%) was observed at 35°C and 4% protein content, while the highest recovery for WP80 (58.53 ± 2.92%) was obtained at 5°C and 12% protein content. For MPC80, the temperature influenced the %R without any particular trend, varying from 69-86, 15-54, and 14-23% at a protein content of 4, 10, and 12%, respectively. Similar trend was observed for ICM formulated with WPC80, where the %R values varied from 20.32-50.32, 16.83-40.85, and 10.85-58.53% at

a protein content of 4, 10, and 12%, respectively. On the other hand, the %R values significantly decreased with the protein content for ICM formulated with MPC80. This behavior was observed at all tested temperatures. At 35°C, for instance, the %R decreased from  $86.97 \pm 4.34$  to  $15.99 \pm 0.89$ , and  $14.94 \pm 1.01\%$  at 4, 10, and 12%, respectively. For WPC80, the %R values varied within a narrower range compared with that of MPC80, and such variation did not display any trend.

The Burger model (Equation (11)) was used to analyze the experimental curve within the creep phase (**Table 3** and **4**). Ice-cream mixes formulated with MPC80 were satisfactorily represented by the Burger model, judging by the  $R^2 (>0.96)$ ,  $R_{adj}^2 (>0.96)$ , and E (<6%) values. The exception to this generalization was observed in mixes containing 10% protein (MPC80) and handled at 35°C, where the values of  $R^2(0.903)$  and  $R_{adj}^2(0.898)$  were relatively lower. Similarly, the Burger model has been used to evaluate the impact of temperature and composition on the viscoelastic properties of regular ice-cream mixes (Kurt et al., 2016; Toker et al., 2013).

On the other hand, the Burger models were less accurate in representing the creep-recovery curves in ICM formulated with WPC80 (**Table 4**), judging by the  $R^2(0.84-0.97)$ ,  $R_{adj}^2(0.81-0.96)$ , and E (<7%) values. In this study, the protein content was increased at the expense of the fat content. Therefore, the observed rheological properties are a result of a combined effect of protein and fat content.

**Table 3.** Summary of regression analysis of the Burger model (Equation (9)) for ice-cream mixes formulated with milk protein concentrate 80 (MPC80).

Parameters	4%-MPC80			
	5°C	15°C	25°C	35°C
$J_o$	0.163 ± 0.027	0.285 ± 0.035	0.227 ± 0.033	0.329 ± 0.049
$J_1$	0.317 ± 0.026	0.403 ± 0.033	0.515 ± 0.031	1.55 ± 0.16
$\lambda_{ret}$	14.04 ± 2.64	19.22 ± 3.91	22.77 ± 3.52	62.91 ± 10.94
$\eta_0$	893.5 ± 63.8	937.1 ± 11.5	451.7 ± 27.1	1442.4 ± 149.1
$R^2$	0.972	0.969	0.975	0.980
$R^2_{adj}$	0.971	0.967	0.974	0.979
E(%)	6.36	8.26	5.02	8.28
Parameters	10%-MPC80			
	5°C	15°C	25°C	35°C
$J_o$	0.150 ± 0.031	0.191 ± 0.031	0.291 ± 0.051	0.405 ± 0.145
$J_1$	0.378 ± 0.029	0.707 ± 0.033	0.571 ± 0.048	0.353 ± 0.139
$\lambda_{ret}$	23.81 ± 4.77	30.84 ± 3.84	15.94 ± 3.12	6.06 ± 4.76
$\eta_0$	192.3 ± 4.72	206.4 ± 7.2	158.4 ± 3.97	89.72 ± 2.14
$R^2$	0.979	0.986	0.967	0.903
$R^2_{adj}$	0.978	0.985	0.965	0.898
E(%)	4.50	4.20	4.06	5.06
Parameters	12%-MPC80			
	5°C	15°C	25°C	35°C
$J_o$	0.177 ± 0.003	0.395 ± 0.117	0.541 ± 0.171	0.602 ± 0.158
$J_1$	0.722 ± 0.003	0.931 ± 0.110	0.865 ± 0.162	1.45 ± 0.14
$\lambda_{ret}$	25.91 ± 3.08	16.21 ± 4.49	13.26 ± 5.56	18.29 ± 4.51
$\eta_0$	53.48 ± 0.43	39.33 ± 0.56	33.09 ± 0.57	31.20 ± 0.53
$R^2$	0.998	0.988	0.983	0.986
$R^2_{adj}$	0.998	0.988	0.982	0.985
E(%)	2.76	4.83	5.34	4.82

$J_o$  – instantaneous compliance;  $J_1$  – compliance associated with the Kelvin-Voigt element;  $\lambda_{ret}$  – retardation time associated with the Kelvin-Voigt element;  $\eta_{oM}$  – viscosity of the Maxwell dashpot ;  $R^2$  – coefficient of determination;  $R^2_{Adj}$  – adjusted coefficient of determination; E(%) – average absolute percentage of residuals.

**Table 4.** Summary of regression analysis of the Burger model (Equation (9)) for ice-cream mixes formulated with whey protein concentrate 80 (WPC80).

Parameters	4%-WPC80			
	5°C	15°C	25°C	35°C
$J_o$	0.079 ± 0.028	0.104 ± 0.002	0.204 ± 0.002	0.382 ± 0.008
$J_1$	0.065 ± 0.027	0.117 ± 0.002	0.293 ± 0.002	0.255 ± 0.007
$\lambda_{ret}$	4.25 ± 3.38	6.57 ± 2.28	20.86 ± 4.42	10.93 ± 7.27
$\eta_0$	456.07 ± 9.09	399.9 ± 6.42	227.5 ± 5.13	122.5 ± 3.05
$R^2$	0.921	0.957	0.975	0.904
$R^2_{adj}$	0.916	0.955	0.974	0.899
E(%)	3.90	2.86	2.83	4.41
Parameters	10%-WPC80			
	5°C	15°C	25°C	35°C
$J_o$	0.032 ± 0.007	0.095 ± 0.002	0.093 ± 0.001	0.199 ± 0.061
$J_1$	0.033 ± 0.006	0.069 ± 0.002	0.179 ± 0.002	0.162 ± 0.059
$\lambda_{ret}$	5.18 ± 2.27	6.44 ± 4.05	13.97 ± 2.48	5.67 ± 4.07
$\eta_0$	1697.8 ± 38.18	542.2 ± 12.51	612.3 ± 15.92	215.1 ± 5.1
$R^2$	0.893	0.888	0.971	0.887
$R^2_{adj}$	0.888	0.882	0.969	0.882
E(%)	4.02	3.57	3.88	4.21
Parameters	12%-WPC80			
	5°C	15°C	25°C	35°C
$J_o$	0.161 ± 0.002	0.239 ± 0.074	0.563 ± 0.103	0.994 ± 0.326
$J_1$	0.196 ± 0.001	0.205 ± 0.071	0.554 ± 0.098	0.457 ± 0.312
$\lambda_{ret}$	20.10 ± 4.91	4.65 ± 3.13	10.49 ± 4.01	6.31 ± 8.62
$\eta_0$	612.7 ± 28.2	212.9 ± 5.53	85.58 ± 1.83	46.18 ± 1.29
$R^2$	0.953	0.829	0.941	0.843
$R^2_{adj}$	0.951	0.819	0.938	0.835
E(%)	4.18	4.42	3.10	5.07

$J_o$  – instantaneous compliance;  $J_1$  – compliance associated with the Kelvin-Voigt element;  $\lambda_{ret}$  – retardation time associated with the Kelvin-Voigt element;  $\eta_{oM}$  – viscosity of the Maxwell dashpot;  $R^2$  – coefficient of determination;  $R^2_{Adj}$  – adjusted coefficient of determination; E(%) – average absolute percentage of residuals.

### *Secondary models*

The  $J_o$  values decreased with increasing temperature, while no particular pattern was observed with increasing the protein content. This generalization was observed for both protein sources.  $J_o$  measures the elastic strength of the bonds within the interfacial network (Karaman, Yilmaz, Cankurt, Kayacier, & Sagdic, 2012). Lower  $J_o$  values suggest a network that is less resistant to deformation and relatively free to rearrange when stress is applied. On the other hand, the  $J_1$  values slightly increased with the temperature, and increased with the protein content, being more notorious for ICM formulated with WPC80 (**Table 3** and **4**).  $G_1$  is associated with bond breakages and reformation of the network structure (Dolz et al., 2008). Thus, an increase in the  $G_1$  values with increasing the protein content is associated with a dominant viscoelastic behavior. All mixes exhibited a behavior closer to a viscoelastic material, where  $G_1$  was always larger than  $G_o$ . The  $n_o$  values, a parameter associated with the breakdown of the gel network structure (Razavi, Taheri, & Sanchez, 2013), decreased with the temperature and increased with the protein content for both protein sources. As discussed earlier, caseins micelles are much larger than whey proteins, affecting the colloidal interaction of the mix.

### 3.4 Conclusions

The Burger model was used to analyze through the four-component that represents the Maxwell and the Kelvin-Voigt model. The Burger model in the form of Equation (11) was used to represent the compliance measurements during the creep-recovery curve. All the creep-recovery curves of ICM exhibited a combination of viscous fluid and elastic solid – viscoelastic properties. Overall, creep-recovery curves are associated with the reorientation of bonds within the viscoelastic material. The maximum compliance obtained for MPC80 ( $5.89 \text{ Pa}^{-1}$ ) was considerable higher than that for WPC80 ( $3.63 \text{ Pa}^{-1}$ ) when both mixes contained 12% protein and tested at  $35^{\circ}\text{C}$ . The  $J_o$  values decreased with increasing temperature, indicating a correlation between  $J_o$  and the temperature. With those results we can conclude that the Temperature, protein content as well as the protein source significantly influenced the %R values.

### 3.5 References

- Adapa, S., Dingeldein, H., Schmidt, K. A., & Herald, T. J. (2000). Rheological properties of ice cream mixes and frozen ice creams containing fat and fat replacers. *Journal of Dairy Science*, 83(10), 2224-2229.
- Brito-Oliveira, T. C., Moraes, I. C., Pinho, S. C., & Campanella, O. H. (2022). Modeling creep/recovery behavior of cold-set gels using different approaches. *Food Hydrocolloids*, 123, 107183.
- David, S. A., & Katayama, A. H. (2013). Fractional order for food gums: modeling and simulation.



- Daw, E., & Hartel, R. W. (2015). Fat destabilization and melt-down of ice creams with increased protein content. *International Dairy Journal*, 43, 33-41.
- Dolz, M., Hernández, M. J., & Delegido, J. (2008). Creep and recovery experimental investigation of low oil content food emulsions. *Food Hydrocolloids*, 22(3), 421-427.
- Eisner, M. D., Wildmoser, H., & Windhab, E. J. (2005). Air cell microstructuring in a high viscous ice cream matrix. *Colloids and Surfaces A: Physicochemical and Engineering Aspects*, 263(1), 390-399.
- Faber, T. J., Jaishankar, A., & McKinley, G. H. (2017). Describing the firmness, springiness and rubberiness of food gels using fractional calculus. Part I: Theoretical framework. *Food Hydrocolloids*, 62, 311-324.
- Goff, H.D. (2015). Ice Cream and Frozen Desserts. In Ullmann's Encyclopedia of Industrial Chemistry, (Ed.).
- Goff, H. D. (1997). Colloidal aspects of ice cream—a review. *International Dairy Journal*, 7(6-7), 363-373.
- Huang, W., Liu, H., Lian, Y., & Li, L. (2013). Modeling nonlinear creep and recovery behaviors of synthetic fiber ropes for deepwater moorings. *Applied Ocean Research*, 39, 113-120.
- Karaman, S., Yilmaz, M. T., Cankurt, H., Kayacier, A., & Sagdic, O. (2012). Linear creep and recovery analysis of ketchup-processed cheese mixtures using mechanical simulation models as a function of temperature and concentration. *Food Research International*, 48(2), 507-519.

- Kurt, A., Cengiz, A., & Kahyaoglu, T. (2016). The effect of gum tragacanth on the rheological properties of salep based ice cream mix. *Carbohydrate Polymers*, *143*, 116-123.
- Osorio-Arias, J. C., Vega-Castro, O., & Martínez-Monteagudo, S. I. (2020). Fundamentals of High-Pressure Homogenization of Foods. Reference Module in Food Science; Elsevier BV: Amsterdam, The Netherlands.
- Onyango, C., Mutungi, C., Unbehend, G., & Lindhauer, M. G. (2009). Creep-recovery parameters of gluten-free batter and crumb properties of bread prepared from pregelatinised cassava starch, sorghum and selected proteins. *International Journal of Food Science & Technology*, *44*(12), 2493-2499.
- Rady, A. M., Soliman, S. N., & El-Wersh, A. (2017). Effect of mechanical treatments on creep behavior of potato tubers. *Engineering in agriculture, environment and food*, *10*(4), 282-291.
- Razavi, S. M. A., Taheri, H., & Sanchez, R. (2013). Viscoelastic characterization of sage seed gum. *International Journal of Food Properties*, *16*(7), 1604-1619.
- Regand, A., & Goff, H. D. (2003). Structure and ice recrystallization in frozen stabilized ice cream model systems. *Food Hydrocolloids*, *17*(1), 95-102.
- Sim, J. Y., Enteshari, M., Rathnakumar, K., & Martínez-Monteagudo, S. I. (2021). Hydrodynamic cavitation: Process opportunities for ice-cream formulations. *Innovative Food Science & Emerging Technologies*, *70*, 102675.
- Sozer, N. (2009). Rheological properties of rice pasta dough supplemented with proteins and gums. *Food Hydrocolloids*, *23*(3), 849-855.

- Toker, O. S., Karaman, S., Yuksel, F., Dogan, M., Kayacier, A., & Yilmaz, M. T. (2013). Temperature dependency of steady, dynamic, and creep-recovery rheological properties of ice cream mix. *Food and Bioprocess Technology*, 6(11), 2974-2985.
- Xu, Y. L., Xiong, S. B., Li, Y. B., & Zhao, S. M. (2008). Study on creep properties of indica rice gel. *Journal of Food Engineering*, 86(1), 10-16.

## Chapter 4

### Conclusions

#### 4.1. Overall conclusions

Over the last few years, dairy proteins have become a popular ingredient due to numerous health benefits associated with their consumption, including promoting satiety, appetite control, and exercise recovery. As a result, concentrates and isolates of milk proteins are commonly used to formulate beverages, snacks, dietary supplements, and desserts.

Consumers hold a special appeal for frozen desserts as they provide a suitable source of protein. Currently, the manufacture of high-protein ice cream is an area of industrial interest. However, the formulation of such ice cream is not a trivial task. Applying the same concepts of Greek-style frozen desserts result in technical challenges such as compatibility of ingredients, mixing, formulation, freezing, and handling the changes in flow characteristics. This research project aimed at studying the effect of temperature (5, 15, 25, and 35°C) on the rheological behavior of the different high-protein ice-cream mix (HP-ICM) samples made from milk protein concentrate (MPC80), Whey protein concentrate (WPC80) with 3 different protein percentages (12%, 10%, 4%). The rheological behavior of different samples was evaluated in terms of dynamic, flow, and creep-recovery using a cone and plate configuration on Anton Paar MCR 92 rheometer. It was found that the rheological properties of the ICM were profoundly influenced by the protein source, protein content, and temperature, yielding the following conclusions:

- The viscosity of the ice-cream mixes was modeled using the Herschel-Bulkley model, where the consistency index was parametrized to account for the effect of temperature and protein content.

- The mechanical spectra of the ICM suggested a stronger elastic structure with increasing the protein content.
- The Burger model satisfactorily described the creep phase of the different ICM, whereas the recovery phase was described by an empirical model.

The protein content negatively impacted the percentage of recovery, according to the creep-recovery test.

The outcomes of this investigation provide opportunities for designing freezing strategies for high-protein frozen desserts.